Historical Channel Locations of the Nooksack River

Report to

Whatcom County Public Works Department
322 N. Commercial St., Suite 120
Bellingham, Washington

Brian Collins and Amir Sheikh
Department of Earth & Space Sciences, University of Washington
Seattle, WA 98195

November 23, 2004

CONTENTS

LIST OF FIGURES

LIST OF TABLES

SCOPE

This report documents historical channel positions for the Nooksack River from the river's mouth to RM (river mile) 58 near the town of Glacier on the North Fork, the Middle Fork to Middle Fork RM 5 (Heislers Creek above the Mosquito Lake Bridge) and the South Fork to South Fork RM 16 (downstream of the Skagit County line). [All river miles refer to river miles marked on USGS 7.5 minute topographic maps.] Channel positions are from 15 sets of orthorectified aerial photos from 1933 through 2000, USGS topographic maps from 1906-1918, and General Land Office plat maps from 1859-1897. Photographs were orthorectified, and maps were georeferenced, brought into a GIS, and channel features were digitized from the photos and maps. Digital data accompanying this report include these maps, photos, and GIS layers made from them. The report includes two analyses of channel position change in the 1859-2002 period covered by the data described above. The first examines the lateral change in position of channel centerlines for each time interval, measured along 525 transects made orthogonal to the floodplain centerline, at 200-m intervals. The second uses a grid analysis to characterize the spatial and temporal pattern with which the river channel occupies the floodplain.

GEOLOGIC AND TOPOGRAPHIC CHARACTERISTICS OF THE NOOKSACK RIVER VALLEY

For the study area, we mapped the extent of the valley bottom, and valley bottom landforms (e.g. floodplain, terraces, alluvial fans, and large landslides) using a combination of published geological mapping (Easterbrook 1976; Dragovich et al. 1997; Lapen 2000) and interpretation of elevations from a DEM created from Whatcom County Public Works elevation data. For analysis purposes we divided the study area into 12 segments parts (Table 1 and Figure 1). The geological history shapes the river bottom morphology and landforms in these different segments, as described below.

Nooksack Delta (RM 0-RM6). The greater Nooksack River delta includes the historic Lummi River and the Nooksack River. At the time of earliest British and Euro-American exploration and Euro-American settlement, the Lummi River channel was the dominant distributary channel; this is shown on early Boundary Survey maps, and described by early U. S. Coast & Geodetic Survey (USC&GS) surveyors (Gilbert 1887) and in early investigations by the U. S. Army Engineers (Habersham 1881; Ogden 1895). Over the course of the delta's development, substantial flow of water and sediment would have routed to both sides of the delta. The outer limit of tidal marsh on the Nooksack River delta has prograded (built seaward) roughly 2 km between the first detailed (USC&GS) map in 1887 (see Table 2) and 1998. In the early 20th century, the Nooksack avulsed from one distributary to another several times, in some cases assisted by settlers (Deardorff 1992). The Nooksack River has been partially diked beginning in the 1920s (Deardorff 1992). For this analysis we divided the delta into a lower segment (RM 0-RM2), which includes the avulsing distributary channels, and an upper segment (RM 2-RM 6, at the I-5 bridge near Ferndale) lacking distributary channels other than the Lummi River.

Lower Nooksack (RM 6-RM 20). The lower Nooksack valley (upstream of Ferndale and downstream of Everson) is broad, ranging in width between 0.7 and 4.5 km (Figure 2), and inset within low-relief hills underlain by glacial sediments. This broad, gently sloping valley was likely formed by runoff from the lobe of the Cordilleran ice sheet that entered the lower Nooksack through the Sumas River valley

(Dragovich et al. 1997). Riverbanks and natural levees are higher than the surrounding floodplain, which drops in elevation with distance from the channel, typically by 3-4 m below the riverbanks (Figure 5A; the profiles in Figure 5 were made by sampling a DEM made from data provided by Whatcom County Public Works, at 2 m intervals). The channel gradient varies between about 0.001 and 0.0001. We subdivided the lower Nooksack into two segments on the basis of different historical channel migration characteristics and rates (see later in report). Levees were built along the lower Nooksack, beginning primarily in the 1930s. Levees are not widespread elsewhere in the study area outside of the delta or lower Nooksack. We divided the lower Nooksack into a lower segment (RM 6-RM15) in which the channel is slightly sinuous and lacks much channel migration and an upper segment (RM 15-RM 20) in which the channel historically was meandering and had a meander belt several times the channel width (see later in the report).

Upper Nooksack (RM 24-RM 37). Upstream of Everson and downstream of the forks, the valley is steeper and narrower than the lower river (Figure 2), ranging in width between 0.3 and 2.3 km. The cross-valley profile contrasts to that of the lower Nooksack (Figure 5B); elevation differences of 3-4 m on the valley bottom are associated with current or former channels, sloughs, and forested islands. Based on ongoing work in Puget Sound river valleys, we assume the difference between the lower and upper Nooksack reflect their contrasting Holocene aggradational and degradational regimes, respectively. We also delineated a "Middle Nooksack" (RM 20-RM 24) segment between the Lower Nooksack 2 and Upper Nooksack 1 segments in which channel dynamics and channel and valley morphology were transitional between the lower and upper Nooksack. We divided the upper Nooksack into a lower segment (RM 24-RM 31) having historically high migration rates and a wide historic channel occupation zone, and an upper segment (RM 31-RM 37) in which migration rates were somewhat less and the occupation zone somewhat narrower than the lower segment (but still sharply contrasting sharply in morphology and dynamics with the lower Nooksack).

South Fork Nooksack (SF RM 0-SF RM 16). The South Fork valley is nearly as wide as, but steeper than, the valley of the lower Nooksack River (Figure 2). The large landslide from Slide Mountain, likely late Holocene in age (Dragovich et al. 1997), constricts the South Fork floodplain (i.e., the valley bottom exclusive of terraces, alluvial fans, and landslide deposits) to about 0.5 km immediately above the confluence with the North Fork. Upstream the floodplain widens to about 2.5 km. The floodplain cross-section varies systematically with distance along the valley. In the first few miles above the Slide Mountain landslide deposit, the river channel is higher than the floodplain by about 1 m at RM 2.7, by about 0.5 m at RM 4.6, and roughly at the same height as the floodplain by RM 6.8 (Figure 5C). This may reflect the constricting effect of the Slide Mountain landslide, which could have induced deposition along the channel; this is speculative. The floodplain east of the river in the lower South Fork is lower in elevation than the riverbanks, which could have favored formation of the historically extensive wetlands in the Black Slough area. The upper South Fork valley steepens between about Acme and Saxon Bridge, and the floodplain's cross-section reflects the "corrugated" topography apparent in the upper Nooksack. Above Saxon Bridge the valley narrows to about 400 m and is constrained by valley walls; this part of the study area has been broken into a separate segment (SF RM 13-SF RM 16).

North Fork Nooksack (RM 37-RM 58). The valley and channel gradients (Figures 2 and 3, respectively) continue to steadily increase from the upper Nooksack through the North Fork Nooksack. The valley bottom is narrower than the upper Nooksack, on average (Figure 2), but the floodplain width varies considerably along the North Fork. The floodplain is widest (about 1,200 m) in the approximately three-river-mile-long segment downstream of the Middle Fork confluence (Figure 1), and is split into a separate segment in this analysis (RM 37-RM 40). Upstream of the Middle Fork confluence, a large Holocene landslide at about RM 44 on the North Fork, similar in size and age to the landslide on the South Fork (see Dragovich et al. 1997), blocked the North Fork valley and now narrows it to only 70 m at the narrowest spot (at approximately RM 43.6). Upstream of this landslide constriction and to about RM 52 the floodplain alluvial and glacio-fluvial terraces narrow the floodplain (Figure 1). For the most part

upstream, mountain slopes confine the valley. The North Fork channel braids, which presumably reflects a river's large load of coarse sediment. Similar to the historic transition in the upper Nooksack, the map and photo record river pattern suggests it has changed from a more branching pattern in the earliest map records to its current braided pattern.

Middle Fork Nooksack (MF RM 0-MF RM 5). The Middle Fork is the steepest and narrowest of the study area's river valleys (Figure 2), the channel gradient is steeper than other channel segments, and the channel gradient undergoes a rapid decline (Figure 3). Low terraces of lahar sediments (Lapen 2000) restrict the floodplain in the lower three river miles (Figure 1). Currently the Middle Fork is substantially wider than shown on earlier map records, and has a primarily braided pattern.

Table 1. Analysis segments used in this study. River miles are continuous along the Nooksack and North Fork Nooksack rivers; separate river mile systems exist on the South Fork and Middle Fork rivers.

RIVER MILE (RM)	SEGMENT	LOCATION
RM 0—RM 2	Delta 1 (DL1)	Mouth to Smuggler Slough
RM 2—RM 6	Delta 2 (DL2)	Smuggler Slough to I-5 bridge at Ferndale
RM 6—RM 15	Lower Nooksack 1 (LN1)	I-5 bridge at Ferndale to Guide Meridian Road bridge
RM 15—RM 20	Lower Nooksack 2 (LN2)	Guide Meridian Road bridge to RM 20.4 (relative to RM marks printed on USGS topographic map)
RM 20—RM 24	Middle Nooksack (MN)	RM 20.4 to Everson (HWY 544 bridge)
RM 24—RM 31	Upper Nooksack 1 (UN1)	Everson (HWY 544 bridge) to Nugent's Corner (HWY 9 bridge)
RM 31—RM 37	Upper Nooksack 2 (UN2)	Nugent's Corner (HWY 9 bridge) to Confluence
RM 37—RM 40	North Fork 1 (NF1)	South Fork confluence to Middle Fork confluence
RM 40—RM 58	North Fork 2 (NF2)	Middle Fork confluence to Glacier
MF RM 0—MF RM 5	Middle Fork (MF)	Confluence to near Mosquito Lake Rd. bridge
SF RM 0—SF RM13	South Fork 1 (SF1)	Confluence to near Saxon bridge
SF RM 13—SF RM16	South Fork 2 (SF2)	Saxon Bridge to near County line

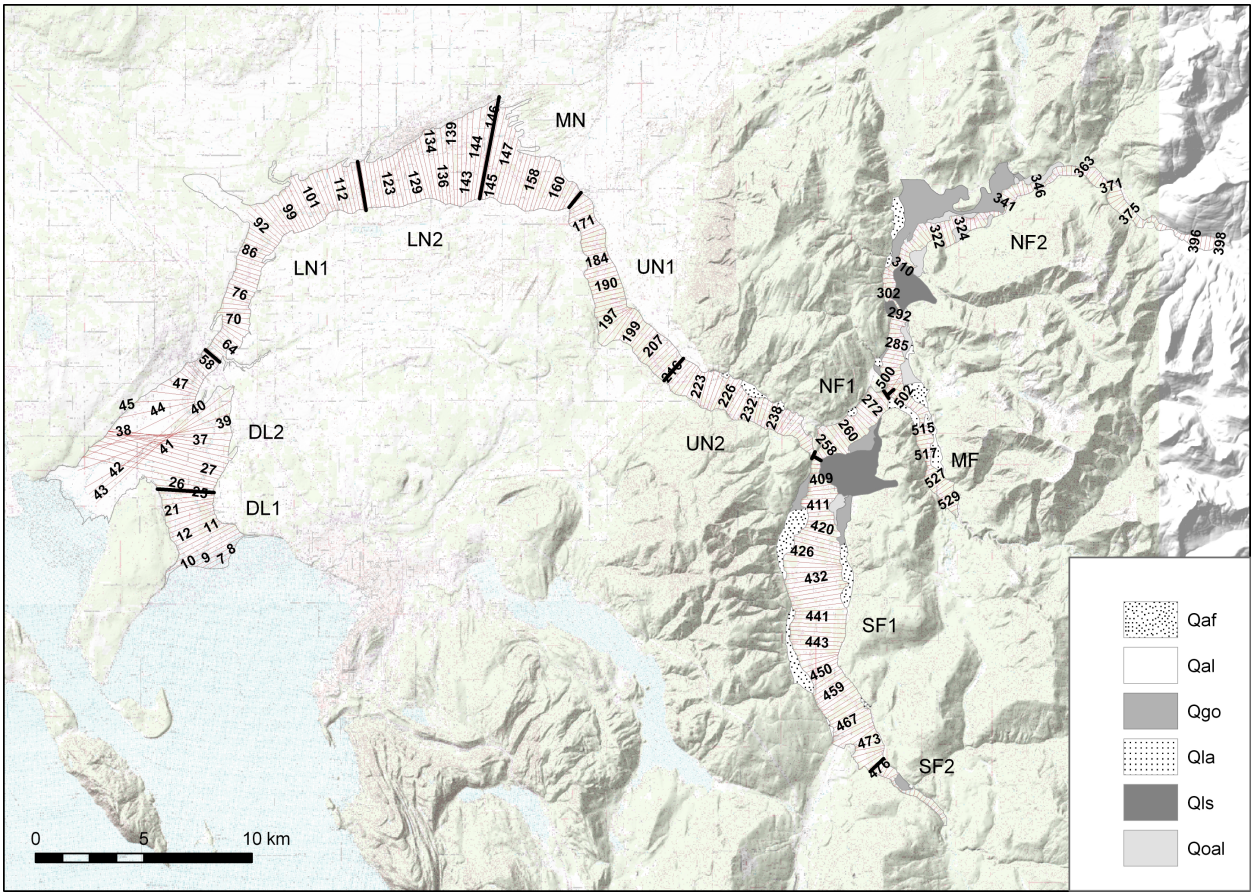

Figure 1. Geology of the study area, location of floodplain transects (numbered), and end points of study segments (Table 1), marked by cross marks. Qal = floodplain; Qaf = alluvial fan; Qgo = glacial outwash terrace (in North and South Forks of the Nooksack); Qla = lahar terrace (in Middle Fork Nooksack River valley); Qls = large Holocene landslide deposits (in North Fork and lower South Fork river valleys); Qoal = Holocene fluvial terraces. Transect numbers are referred to in succeeding figures.

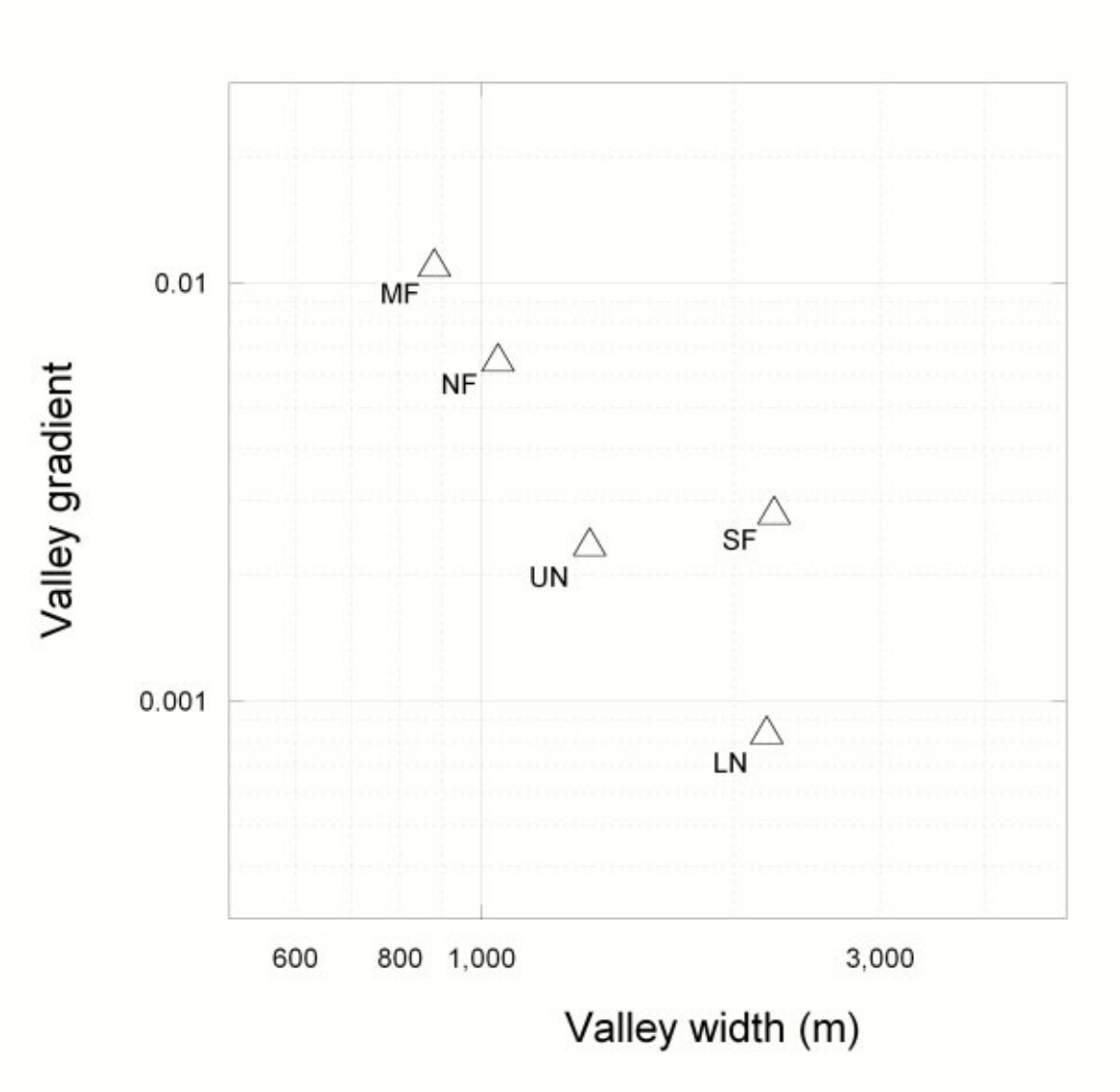

Figure 2. Valley width and valley gradient for the lower Nooksack (NL), Upper Nooksack (UN), South Fork (SF), North Fork (NF), and Middle Fork (MF) valleys. The valley width used in this figure includes the floodplain, terraces, and alluvial fans. Two large Holocene landslides in the North and South forks of the Nooksack are excluded.

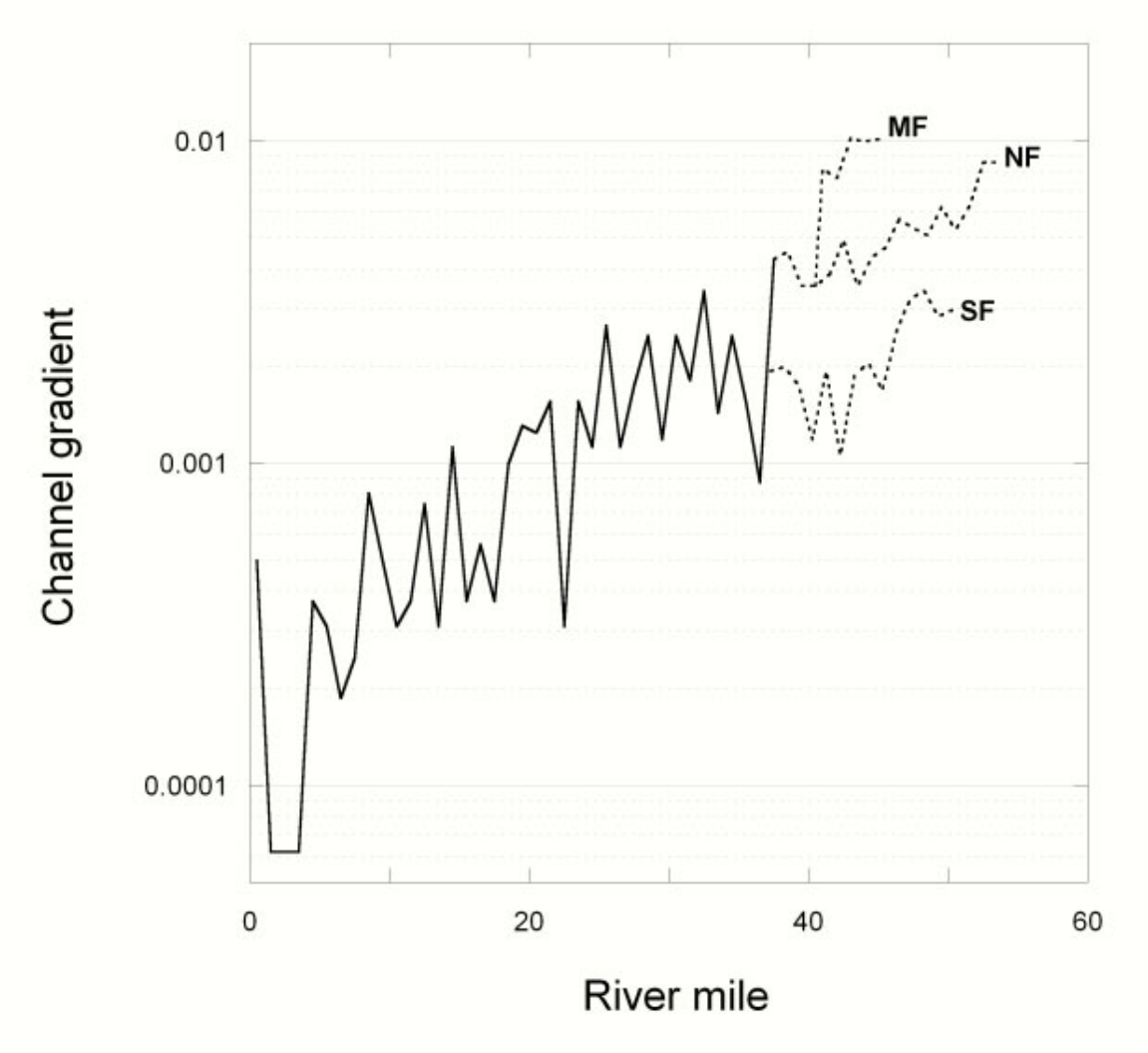

Figure 3. Average channel gradient, measured relative to River Mile marks on USGS 1:24,000 scale topographic maps, and elevations measured at 0.5 mile intervals from DEM described elsewhere in report.

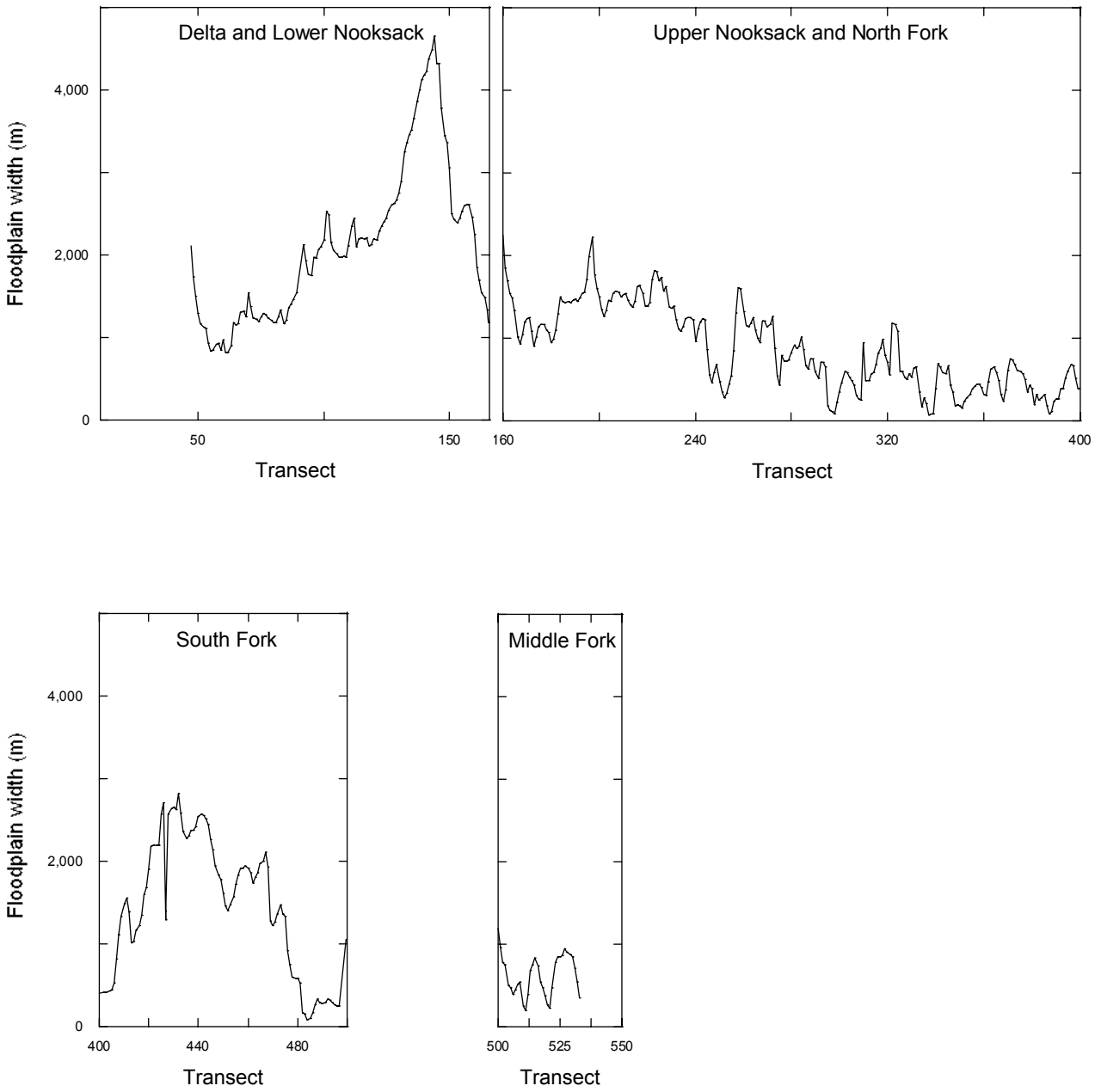

Figure 4. Floodplain width, in meters. Transect numbers refer to Figure 1. Scale of vertical and horizontal axes is the same in each panel. Transects 5-46 on delta (see Figure 1) have been excluded.

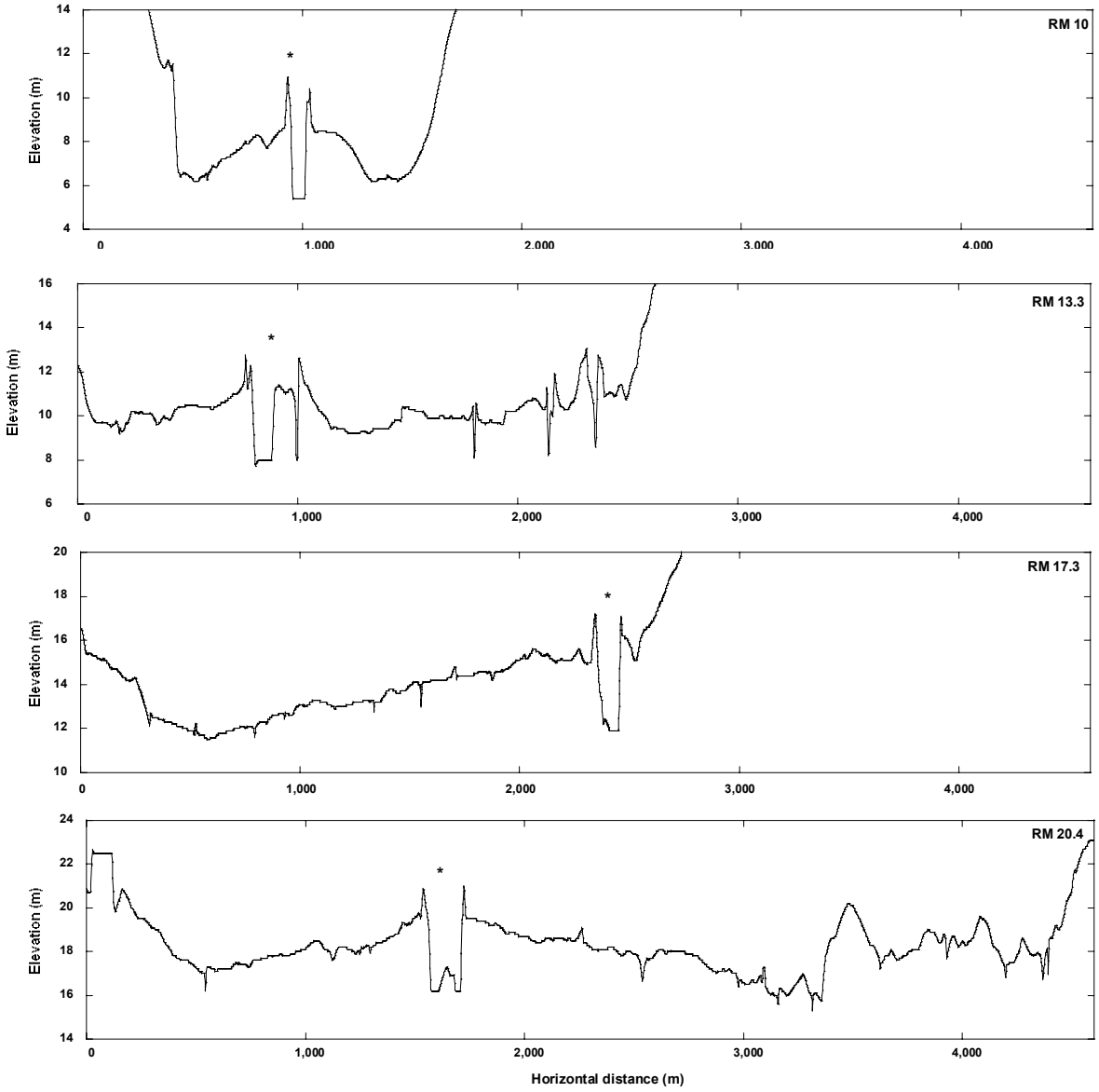

Figure 5A. Representative valley cross sections in the lower Nooksack River mainstem (RM6—RM24). Cross sections were created by sampling 2.5-m-cell size DEM created from 1993 photogrammetric data. "*" = Nooksack River; "+" = road. Vertical exaggeration = 100x.

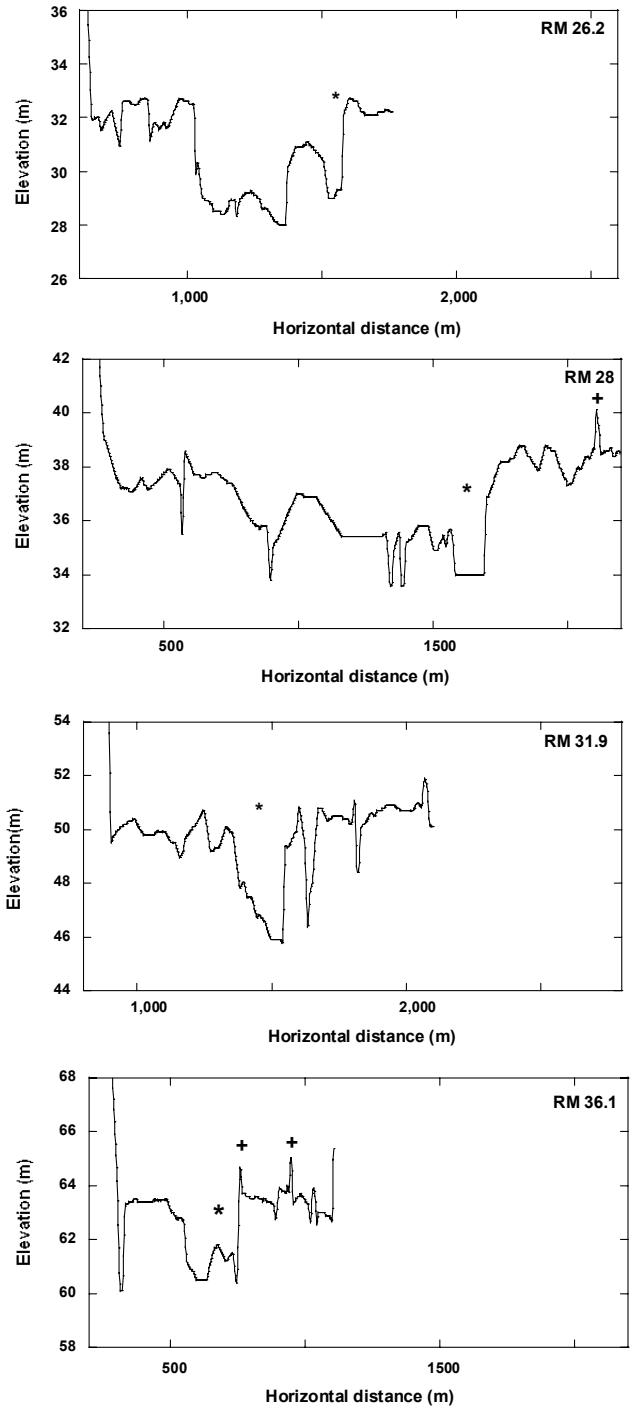

Figure 5B. Representative valley cross sections in the upper Nooksack River mainstem (RM24—RM37). Cross sections were created by sampling 2.5-m-cell size DEM created from 1993 photogrammetric data. "*" = Nooksack River; "+" = road. Vertical exaggeration = 100x.

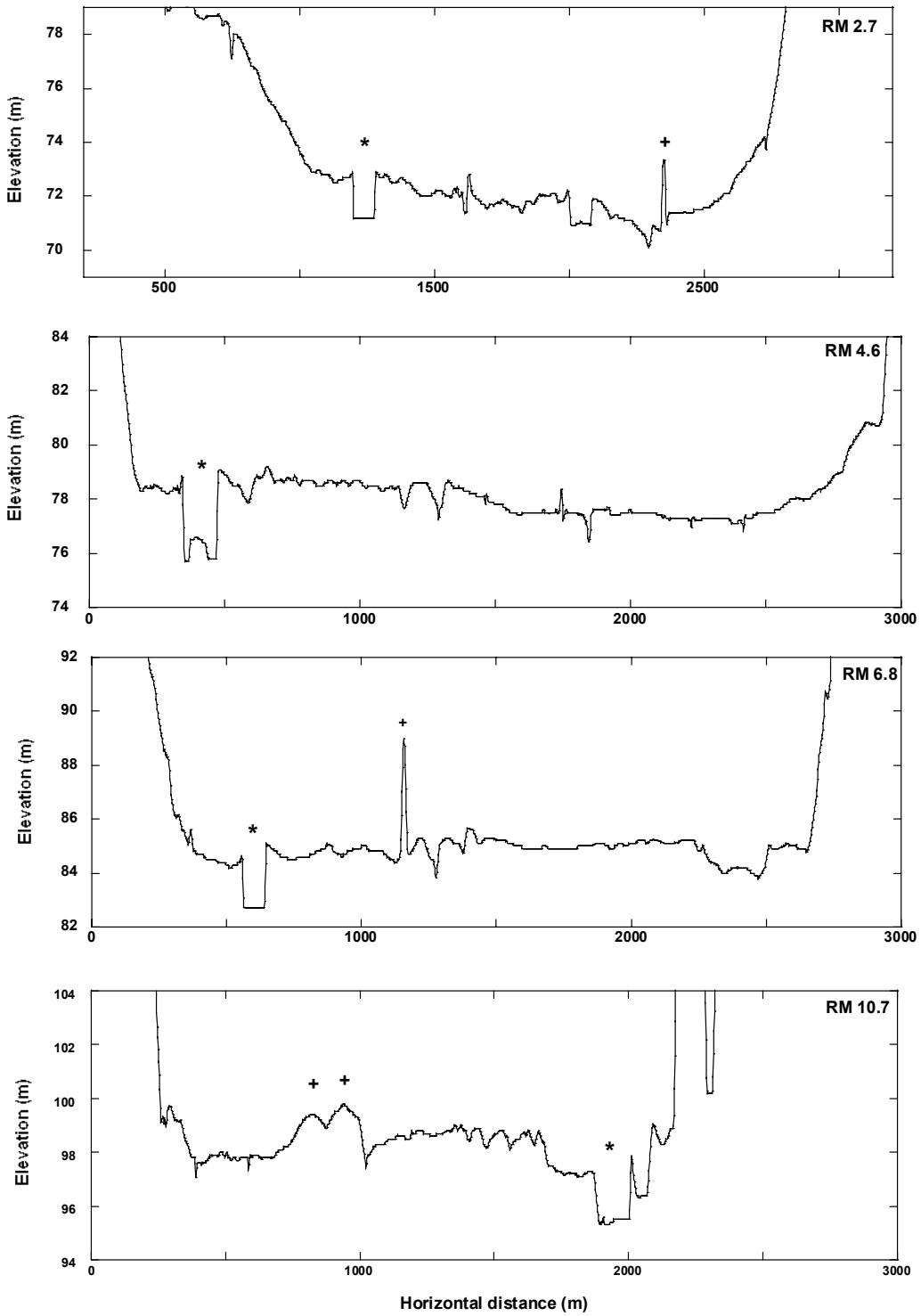

Figure 5C. Representative valley cross sections in the South Fork Nooksack River. Cross sections were created by sampling 2.5-m-cell size DEM created from 1993 photogrammetric data. "*" = Nooksack River; "+" = road or railroad. Vertical exaggeration = 100x.

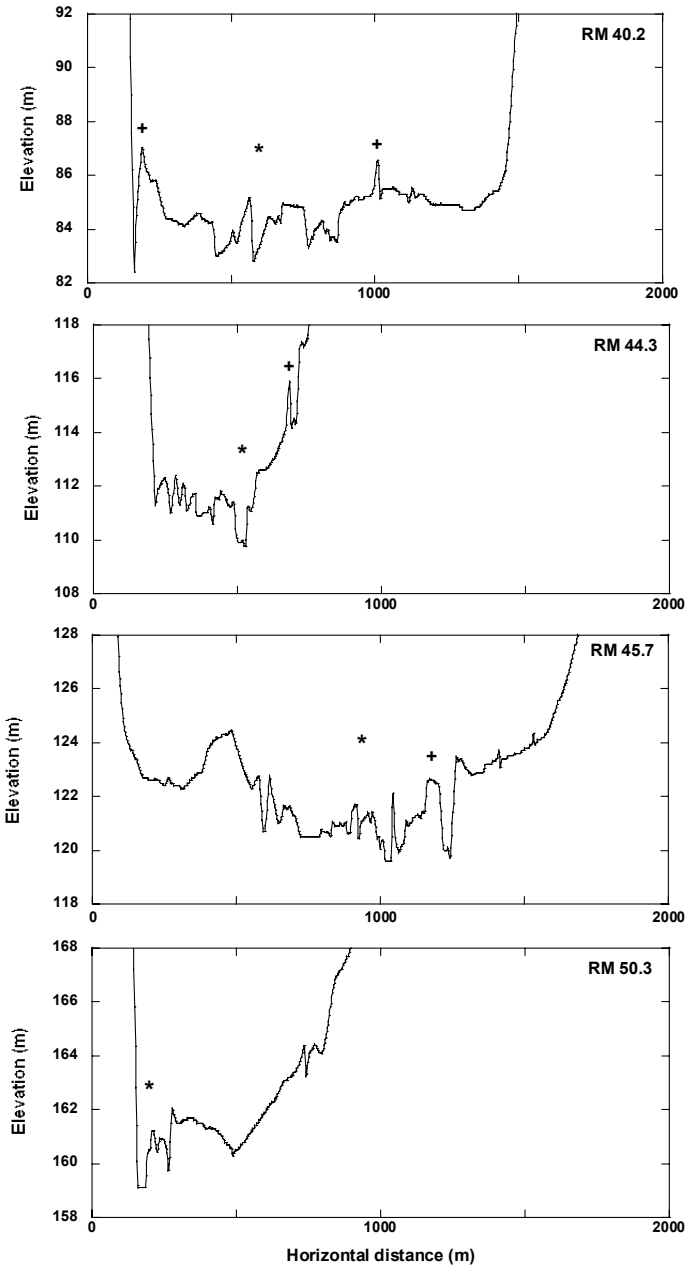

Figure 5D. Representative valley cross sections in the North Fork Nooksack River. Cross sections were created by sampling 2.5-m-cell size DEM created from 1993 photogrammetric data. "*" = Nooksack River; "+" = road or railroad. Vertical exaggeration = 100x.

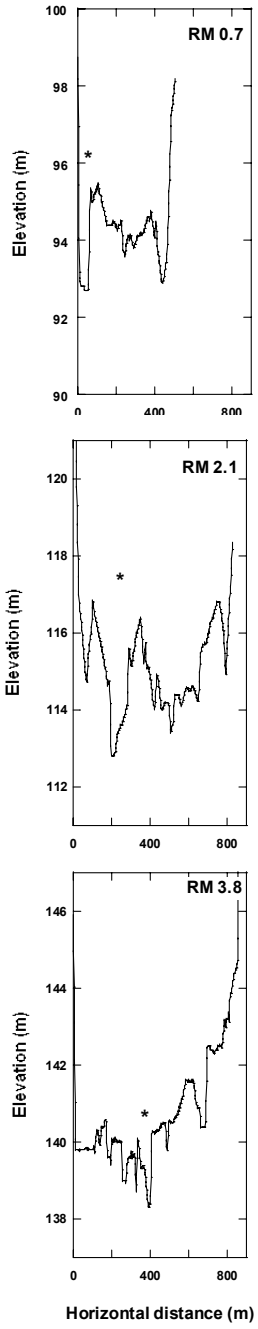

Figure 5E. Representative valley cross sections in the Middle Fork Nooksack River. Cross sections were created by sampling 2.5-m-cell size DEM created from 1993 photogrammetric data. "*" = Nooksack River; "+" = road or railroad. Vertical exaggeration = 100x.

METHODS

Aerial Photos and Maps

We collected aerial photos and maps for the study area, aiming for an average spacing between photo sets of 5 to 10 years. We made use of 15 photo sets between 1933 and 2002 (Table 2), and cadastral and topographic maps between 1859 and 1918 (Table 3). The number of years between maps prior to the earliest photographs (1933) was greater than the time between photographs (Figure 6). Because maps and photos did not always cover the entire study area, some periods between photographs or maps differed between parts of the study area (Figure 6).

The early General Land Office plat maps were our earliest map source. These maps are from surveys conducted in 1859-1897. The delta was surveyed in 1859, the lower Nooksack in 1871-1874, the upper Nooksack in 1884-1885, the South Fork in 1884-1885, the Middle Fork in 1885 and 1890, and the North Fork between 1890 and 1897 (Table 2). We used scans made of original plat maps, available in digital form from the Bureau of Land Management, georeferenced them using the current Public Land Survey System (PLSS) records for corners and quarter corners, then digitized channels from these georeferenced images. From working with channel representations on plat maps elsewhere we have concluded that the mapped channel outline represents the high flow channel (or active channel) rather than the low-flow channel. The instructions to surveyors in use at the time (see White 1991) support this interpretation. Surveyors were instructed to survey "both banks" at the "ordinary mean high water mark;" an early court case defined the ordinary high water mark as "river bed which the river occupies long enough to wrest it from vegetation."

General Land Office surveyors meandered (measured with bearings and distances) navigable rivers including the Nooksack. Our experience is that the horizontal accuracy of the channel location is most reliable where a section line crosses the river. Channels drawn on plat maps were drawn from survey

notes, and channel depictions are sometimes artificially and noticeably geometric in their representation. In North Puget Sound rivers, we found that surveyors drew channels on plat maps with varying fidelity to the field-measured widths, but on average, the GLO cartographers exaggerated widths on the plat maps by a few percent (Collins and Sheikh 2003).

We obtained and then georeferenced gray-scale scans of USC&GS topographic sheets (T-sheets) from the U. S. Library of Congress. T-sheets do not reference a current datum (i.e. NAD 27, NAD 83). Instead they have graticules marking latitude and longitude in the early local Puget Sound Datum (PSD); a later update to North American Datum (NAD) projection is also often present. To calculate the X, Y shift from NAD to NAD 27 necessary to georeference the images, X and Y values were used from datum difference tables, created from the resurvey early in the 20th century of survey stations around most of Puget Sound (Patton, 1999). We determined an overall datum shift for the area covered by a T-sheet by averaging the shift from a number of survey stations in or nearby the area represented on the T-sheet. In calculating this shift, in general RMS values were .003 or below, and points that produced RMS errors above .003 were discarded through an iterative process. To provide an independent check on the accuracy of the registration process (not the accuracy of the original survey itself), benchmarks located on the T-sheets were compared to published NGS benchmarks that were retraceable to the time of the surveyed T-sheet. The accuracy assessment only made use of benchmarks which could be established with a high degree of certainty to have existed at the time of the original T-sheet survey, and which had not been remounted. It was not possible to make this accuracy check on T-1798 used in this study (see Table 2); accuracy of the georeferencing process for 1:10,000 scale T-sheets such as T-1798 elsewhere in Puget Sound ranged from 2 to 8 meters.

We scanned USGS 62,500-scale topographic maps from 1906 and 1918 (Table 2A), and georeferenced them using current PLSS records. These early topographic maps have considerably less horizontal accuracy than modern topographic maps, and less horizontal accuracy than the aerial photographs we used.

All photo sets were paper prints, which we scanned at 600 ppi [except for USGS 1998 digital orthophoto quarter quadrangles (DOQQ)]. Photo scale varied from 1:4,800 to 1:24,000, with one set at a much smaller scale (1980, scale 1:58,000). The 1998 USGS DOQQs have a horizontal resolution of 1m. All photo series were black and white except 1980 (false color) and 1976 and 2002 (color). We orthorectified all photographs, with ERDAS Imagine Orthobase, using the 1998 USGS DOQQs and a USGS 10-m DEM. We then mosaiced and tiled the orthorectified images. We did not perform an independent test of the accuracy of orthorectified imagery.

Digitizing

We digitized channel features heads-up on-screen in ESRI ArcGIS, at an approximate scale of 1:1,000. We mapped the active channel using the map units listed in Table 4. We designated the wetted channel at the time of the photos the "low flow channel" (coded as LF). Areas mapped as "high flow" (coded HF) are generally unvegetated but include patches of shrubby or immature forest vegetation. We considered these two units together as the "active channel." We mapped a vegetation patch as a "forested island" (coded FI) if the patch included mature trees, particularly mature conifers, these mature trees being taken as a surrogate for surfaces that had accreted vertically high enough to function as floodplain rather than gravel bar. We mapped the channel from General Land Office plat maps, as "active channel" (coded as AC), encompassing the low flow and high flow channel (Table 4), and also used "FI" for forested areas between major flow splits shown on the plat maps.

The accuracy with which the channel could be digitized varied with the scale and quality of aerial photos and with the presence or absence of streamside trees. For years from larger-scale photography (1:12,000 scale or larger), the error in digitizing channel features not obscured by vegetation or by glare is small when averaged over a few tens of meters. However, in locations on the same photographs where the channel margin is overhung by vegetation or the photographs have sun glare, we estimate a typical potential error to be $\pm$ 3 m. On the smaller-scale photography (1:12,000-scale or smaller), we estimate a

typical error caused by vegetation cover or glare can locally be as much as $\pm$ 5 m. The 1980 photomosaics were the smallest scale photographs (1:58,000), with relatively poor image quality, and the potential maximum error in digitizing channel features from those photos locally could be as much as $\pm$ 7 m; the orthorectification error is also larger for these photographs. The migration analysis made use of centerlines we located visually and digitized heads-up on-screen, and this would also introduce another source of error, although on the other hand the use of the centerline would also tend to smooth out local inaccuracy in digitizing the riverbanks. We do not expect that any of these digitizing errors are systematic, and thus their effect would be to increase the variance of the migration rate data. This is a general assessment of the digitizing error; to assess the local precision of the digitization process, we recommend the user compare the GIS coverages to individual images (e.g. to determine the presence of overhanging vegetation or photo glare).

Channel Migration and Avulsion Analysis

We made two analyses of the channel location data. The first measures the lateral movement of the channel between time periods represented by the maps or photos. We made these measurements by first digitizing a centerline through our floodplain map unit, and then generating cross-valley transects orthogonal to this valley floodplain centerline, at 200 m intervals along the floodplain centerline (Figure 1). As indicated above, we also digitized centerlines through the low flow channel of all data sets. Where there were multiple channels, we chose the largest channel. The migration or avulsion distance between data periods was determined along each of these cross-floodplain transects. The channel migration or avulsion measurements thus reflect change in location orthogonal to the floodplain centerline.

The second analysis characterizes channel location in the period of record as an occupation grid. This analysis was made using digitized layers of the active channel (i.e., low flow channel, gravel bars) and floodplain sloughs for all data periods. We then created grids with a 2 m cell size, and computed the number of times each grid was occupied by the active channel, expressed as a percent.

"Average Annual Migration" in Theory and Practice

Historical *average annual* channel migration rates, for practical reasons, are subject to unavoidable biases. Truly unbiased average annual migration rates can only be computed from aerial photographs or maps made *annually*. Such a record rarely exists, and it does not exist for the Nooksack River. Instead, average annual rates must be approximated using records made at intervals of time. The longer the period is between successive photo or map record, the greater is the bias. This is because as the number of years increases between photo or map records, the likelihood increases that the full record of the river's activity in that time period will be obscured. For example, a river might migrate (or avulse) toward river right in one year, and then toward river left in a second year, and in the third year avulse again toward river right. Photographs taken bracketing this three-year period will only record the net change between the beginning and ending of the bracketing period (which could even result, in the example given here, in zero net migration, and an average annual migration rate of zero), not the actual annual average movement (e.g., in this example, the sum of the river's lateral movement in each year). The greater the time period between photos or maps, the more the measured migration rate underestimates the actual annual average rate. Thus, the longer the time periods used in a study, the more the estimated average annual migration rate will probably underestimate the actual average annual migration rate. This bias toward underestimating is more the case in rivers characterized by frequent channel-switching avulsions, in which the channel is shunted by flood events from the main channel to a former channel, and by the next flood into another channel, because it is more likely that the river will have moved multiple times in opposite directions during a period between maps and photos. Rivers characterized by meandering—the more typical "migration" on which channel migration studies, and the concept of average annual migration have been premised—are likely to have less underestimation bias, because the lateral movement tends to be predictably in one direction ("migration") for a number of years in a row.

A different type of bias is also introduced when time increments are unequal. This problem is unavoidable in this region because in the earlier part of the historical record, prior to the availability of

aerial photos, maps made of sufficient quality, or even maps of any kind, were not made with the frequency at which aerial photographs were later flown. This means that minimum time increments (and the potential to underestimate the "average annual migration rate") are inherently greater in the earlier part of the historical record. In addition, aerial photographs were commonly flown with less frequently in the earlier part of the aerial photographic record than in the most recent few decades.

It is possible to correct for unequal time increments by regressing time increment against migration rate (e.g. Figure 8 in O'Connor et al. 2003) to develop a correction factor. However, this assumes that migration rate and time increment are independent variables, which is not likely the case because time increment correlates with time; in other words, longer time increments occurred in the earlier part of the historical record, and shorter increments in the later part of the record, and migration rates may differ between the two time periods; there is reason to expect that migration rates would have differed through time, on account of the dramatic changes to land uses that occurred throughout the historical record. For this reason, we have not made this correction. Instead, we calculate migration rates both for the entire period of record (1859-2002), and for the aerial photo period of record (1933-2002). The former migration rates (for the entire period) contain larger bias, but include important early data, prior to many land use or river engineering changes. The latter migration rates (for the aerial photo record) is less representative because it is shorter, but it has less inherent bias because the time increments are shorter and more uniform, and it also represents conditions most likely to apply to the near term future, in which land uses and river engineering will be similar to the recent past

For the purposes of this study, the following should be kept in mind:

(1) All average annual estimates are underestimates, necessarily because we do not have data from every year.

(2) The lower Nooksack historically has had a meandering pattern, while the upper Nooksack and much of the channel length in the forks has had a historically anabranching, and currently braided, channel pattern, characterized by channel switching (see later in report). This means for example, that the average

annual estimates are less biased (less of an underestimate) in the lower Nooksack than in the upper Nooksack.

(3) Average annual estimates in the early part of the study period, especially before the first aerial photos in 1933, likely have the greatest underestimate of average annual movement. To a lesser extent, measurement periods early in the aerial photo record represent greater underestimates than more recently.

Table 2. Maps used in study, 1859-1918. Source: 1 = Whatcom County Public Works; 2 = Whatcom County Conservation District; 3 = UW libraries; 4 = US Army Corps of Engineers Seattle District; 5 = Bureau of Land Management; 6 = National Archives.

YEAR	SCALE	MAP NAME	TYPE	AREA	SOURCE
1859-1897	1:31,680	T38N R2E (1859) T39N R2E (1871)	General Land Office plat maps	RM 0-12	5
		T39N R2E (1871) T40N R2E (1872) T40N R3E (1872)		RM12-RM 23	
		T40N R3E (1872) T39N R4E (1884) T39N R5E (1890) T38N R5E (1885)		RM 23-37	
		T38N R5E (1885) T39N R5E (1890) T40N R5E (1891) T40N R6E (1893) T39N R6E (1897) T39N R7E (1892)		RM 37-58	
		T38N R5E (1885) T37N R5E (1885)		SFRM 0-16	
		T39N R5E (1890) T38N R5E (1885)		MFRM 0-5	
1887	1:10,000	North part of Bellingham Bay (T-1798)	US Coast & Geodetic Survey T-sheet	RM 0- 2	6
1906	1:62,500	Blaine	15’ USGS topographic	RM 0-14	3
1906	1:62,500	Sumas	15’ USGS topographic	RM 14-34	3
1918	1:62,500	Wickersham	15’ USGS topographic	SF RM 5-16	3
1918	1:62,500	Van Zandt	15’ USGS topographic	RM 34-54 MF RM 0-5 SF RM 0-5	3

Table 3. Aerial photos used in study, 1933-2002. Source: 1 = Whatcom County Public Works; 2 = Whatcom County Conservation District; 3 = UW libraries; 4 = US Army Corps of Engineers Seattle District; 5 = Bureau of Land Management; 6 = National Archives.

YEAR	APPROX. SCALE	PHOTO PROJECT ID	TYPE	AREA	SOURCE
1933	1:15,000	Wallace Aerial Photography	BW photo	RM 0-51 SF RM 0-13	1
1938	1:12,000		BW photo	RM 0-58 SF RM 0-15	4
1943	1:24,000	--	BW photo	SF RM 0-14 MF RM 0-5	2
1950	1:12,000	--	BW photo	RM 0-47 SF RM 0-2	1
1955	1:24,000	Pacific Aerial Surveys & USASCS BBK-P	BW photo	RM 0-58 SF RM 0-15	2
1961	1:4,800	--	BW photo	MF RM 0-5	1
1966-1967	1:20,000	Pacific Aerial Surveys & USASCS BBK-GG	BW photo	RM 0-58 SF RM 0-16	2
1976	1:24,000	Washington DNR NW-C-76	Color photo	RM 0-58 MF RM 0-5 SF RM 0-8	2
1980	1:58,000	USASCS HAP 80	IR photo	RM 0-49 MF RM 0-5 SF RM 0-16	3
1986	1:4,800	Walker & Associates 594-1010	BW photo	RM 0-58 MF RM 0-5 SF RM 0-16	1
1993	1:10,000	Walker & Associates 594-1010	BW photo	RM 0-22	1
1994	1:10,000	Walker & Associates 594-1010	BW photo	RM 29-58 MF RM 0-5 SF RM 0-15	1
1995	1:10,000	Walker & Associates 594-1010	BW photo	RM 22-36	1
1998	1 m horizontal resolution	Source photos for DOQQs: NW-H-98	BW USGS Digital Orthophoto Quarter Quadrangle (DOQQ)	RM 0-58 MF RM 0-5 SF RM 0-16	3
2002	1:10,000	Walker & Associates 502-0313	Color photo	RM 0-37 SF RM 0-2	1

Table 4. Mapping categories used in digitizing channel features on aerial photographs and General Land Office plat maps.

GEOMORPHIC LOCATION	TYPE CODE	DESCRIPTION
Active Channel	LF	Low flow channel at the time of the aerial photograph.
	GR	Gravel bar. Includes small patches of vegetation.
	AC	Active channel, undifferentiated. Includes LF and GR. Used for General Land Office plat maps and early USGS topographic maps.
Forested Floodplain	FI	Forested island. Patch of trees between branches of active channel.

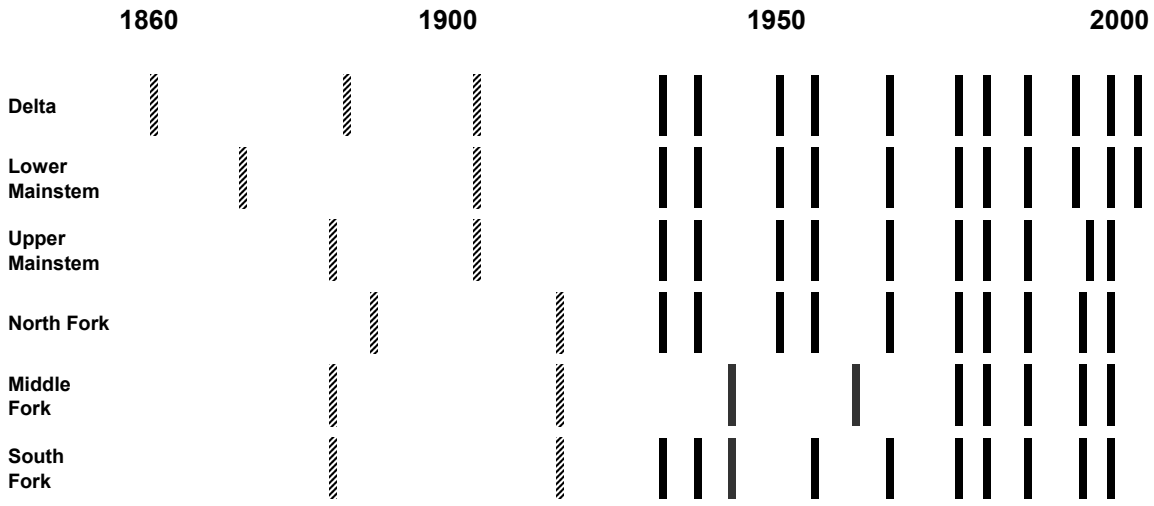

Figure 6. Years of aerial photo (black bar) and map (striped bar) coverage in the delta, lower Nooksack, upper Nooksack, North Fork, Middle Fork, and South Fork.

MIGRATION RATES

Figure 7 shows average annual migration rates, for all time periods, for each floodplain transect. The figure shows the highest rates, and greatest variation in rate, in the upper Nooksack and in parts of the lower North Fork. Anomalously high rates in the lower delta (Figure 7A) reflect several avulsions of distributary channels. The annual rate is time averaged—at each transect, each interval of change is multiplied by the number of years in the interval, this product is summed for all intervals, and the sum is divided by the total time interval at that transect—in Figure 8. Because there is less bias in the data within the aerial photo record (1933-2002, because time increments are smaller and more regular, as discussed earlier), Figure 9 shows migration rates for that period.

Annual migration rate is normalized by channel size for the period covered by aerial photos (Figure 10) by dividing migration rate by the active channel width in 1998 at each transect, giving lateral migration in channel widths per year. This normalization has the effect of reducing the amount of variation in average migration rate that is due to differences in stream width between the different regions of the study area. In other words, while historically the South Fork has migrated less per year than the upper Nooksack or lower North Fork, taking into account that the South Fork is a smaller channel shows that its annual migration rate *relative to its channel size* is comparable to the upper Nooksack or lower North Fork (Figure 10).

Figure 11 shows the mean annual migration for each time period within the twelve study segments. There is generally a large variation in migration rate between time periods, which is expected because the most rapid lateral migration or avulsion occurs during large, infrequent storms. With a few exceptions, there are not systematic trends in the migration rates within study segments. Exceptions include the lower delta segment (DL1; Figure 11A), where earlier rates were higher because of the few avulsions that occurred in the early time period, as mentioned above. The LN1 segment (lower Nooksack between RM 6—RM 15; Figure 11C) shows a trend toward lower rates through time. This could reflect the effects of

bank protection in this segment; however, rates are very low throughout the period of record, in the early part between 2-3 m/yr and in the latter period between 1-2 m/yr. Finally, the Middle Fork Nooksack migration rate systematically increased through time (Figure 11L).

Table 5 lists annual migration rates averaged for the study segments described in Table 1. The three columns in the table show average annual migration rates for the entire period of map and photo record, for the period of map record prior to 1933, and for the period of aerial photo record beginning in 1933. Segment-averaged annual rates varied greatly. The lowest migration, in the 1933-2002 period, was in the Delta 2 and Lower Nooksack 1 segment, which averaged only about 1 m/yr (0.9m/yr and 1.2 m/yr, respectively). The greatest migration was in the North Fork 1 and Upper Nooksack 1 segments, which averaged 17.2 m/yr and 18.5 m/yr, respectively. As discussed earlier, the migration rate in the historically meandering lower Nooksack is likely to be less of an underestimate, while the value for the Upper Nooksack 1 segment is likely to be an underestimate, so that the difference in rate between the two areas is likely even greater than measured.

Table 5 also lists average rates by study segment for the period prior to 1933, and for the period after 1933. In the study segments where rates have been the highest in the post-1933 period (UN1, UN2, NF1, NF2, MF), the post-1933 rates were between 1.8 times and 3.1 times greater than the pre-1933 rates. While the pre-1933 rates are expected to underestimate annual rate because they represent longer time periods than during the aerial photo record, the large difference between the two time periods (factors of 1.8 to 3.1 times greater) is probably much greater than the possible bias, and more likely reflects changed conditions (e.g., differences in bank stability associated with riparian logging; differences in sediment loads; loss of very large pieces of wood to form key pieces in jams to nucleate stable islands) between the two time periods.

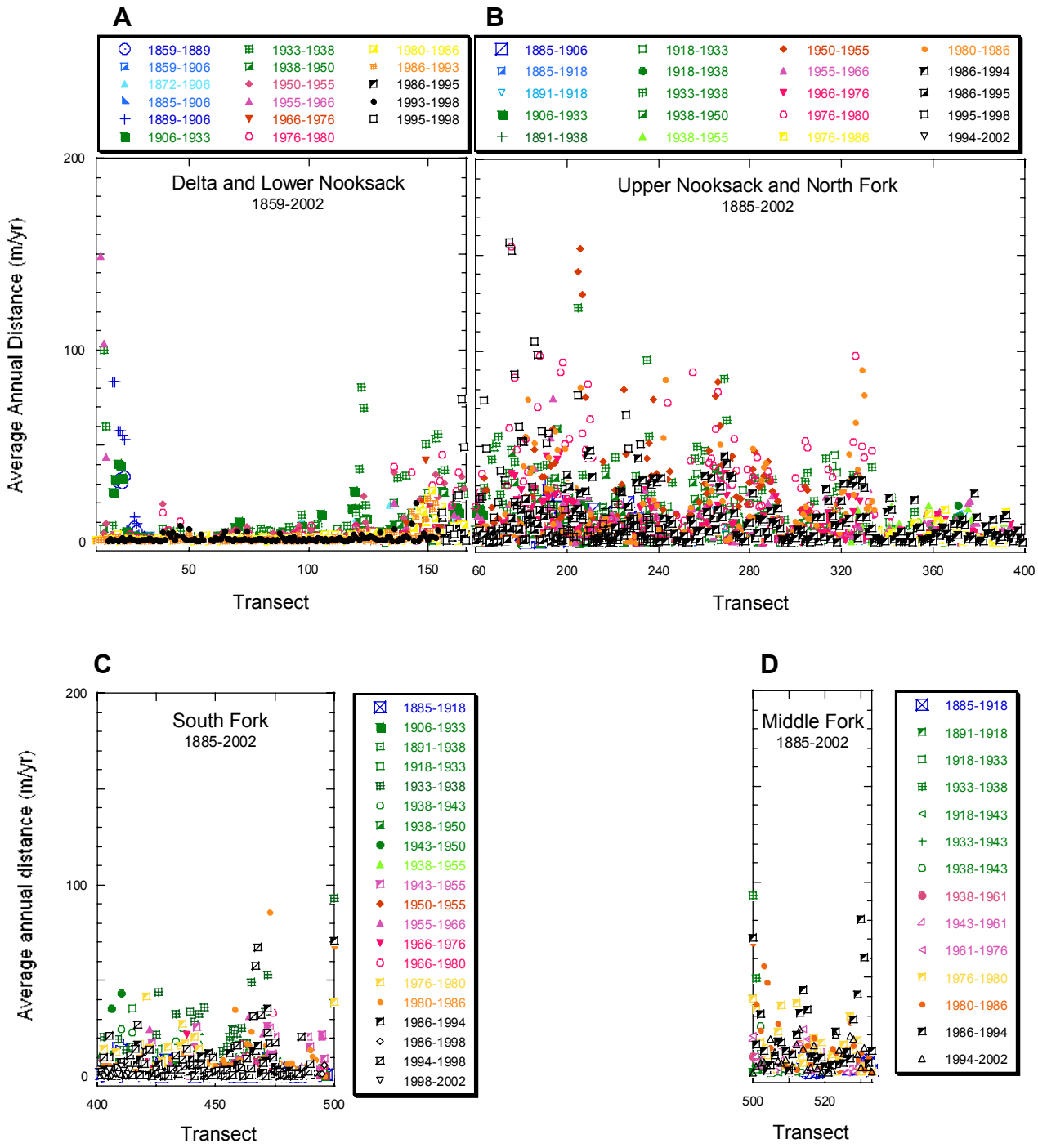

Figure 7. Average annual distance moved by channel centerline for individual time increments, for period of map and photo record. Transect numbers refer to Figure 1. Scale of vertical and horizontal axes is the same in each panel.

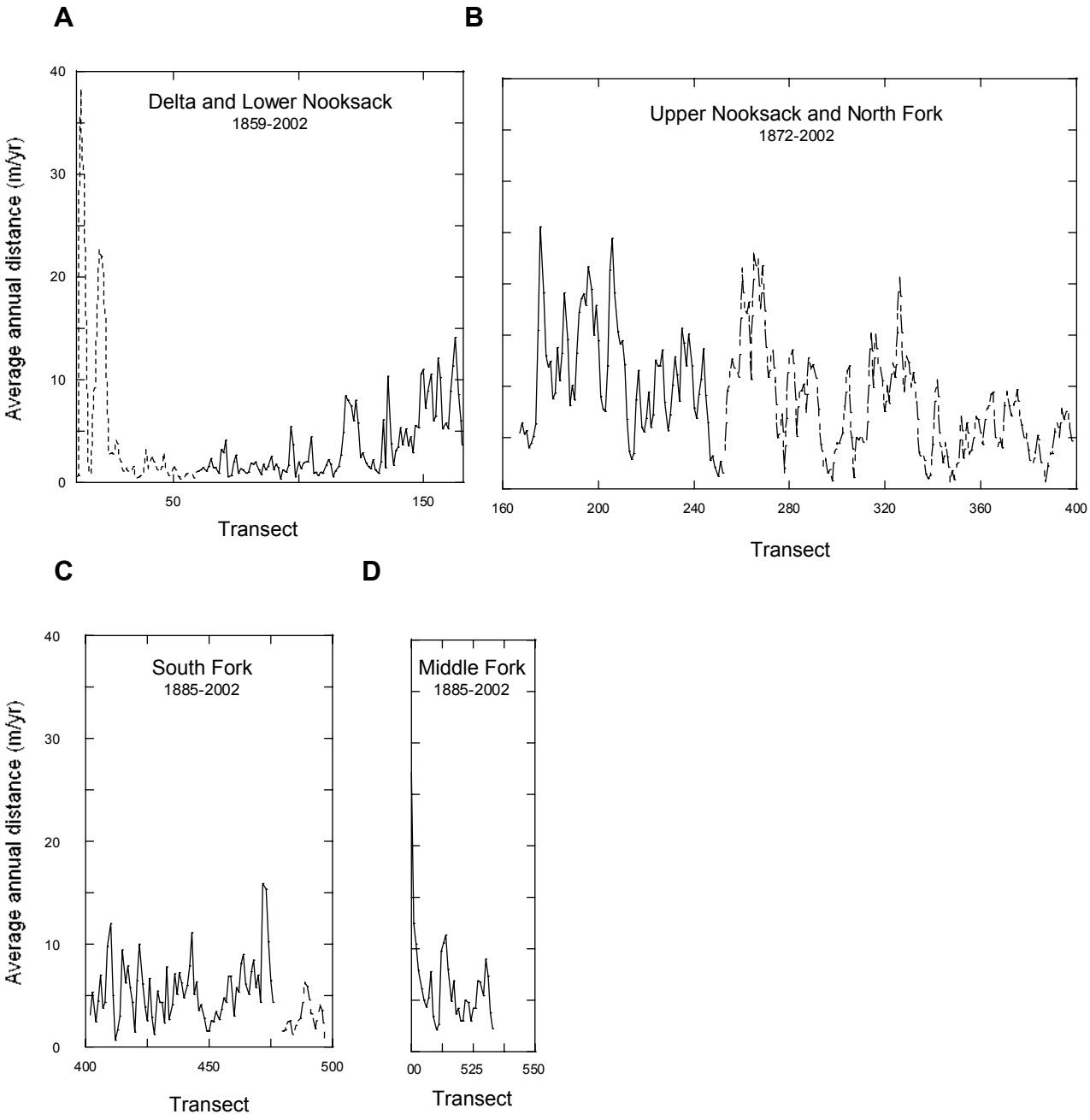

Figure 8. Weighted average annual distance moved by channel centerline for period of map and photo record, in (A) Delta (dashed line) and lower Nooksack (solid line), (B) Upper Nooksack (solid line) and North Fork (dashed line), (C) South Fork (solid line) and upper South Fork (dashed line), and (D) Middle Fork. Transect numbers refer to Figure 1. Scale of vertical and horizontal axes is the same in each panel.

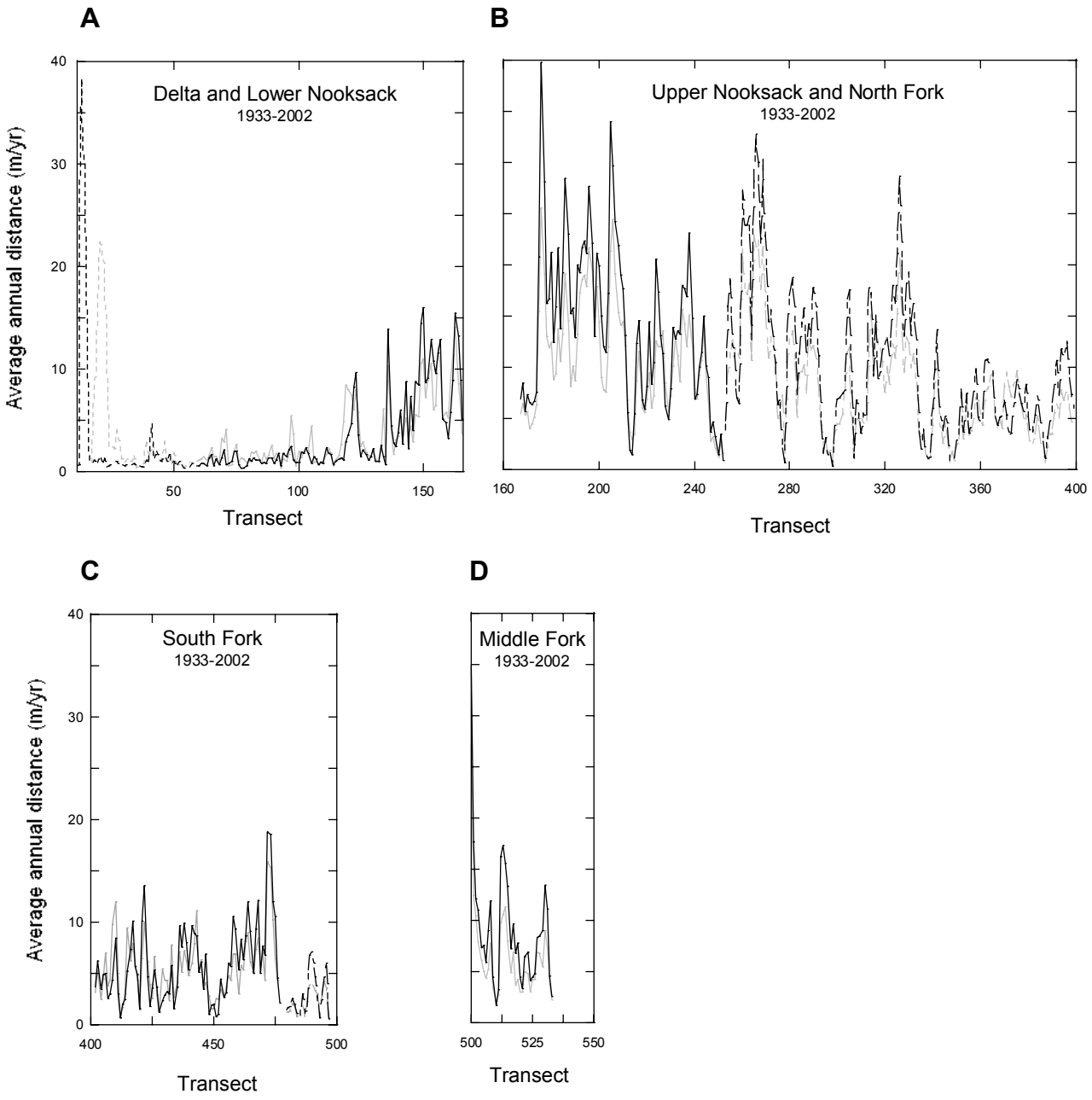

Figure 9. Weighted average annual distance moved by channel centerline since 1933 (average for entire period of record, from Figure 8, shown with gray line), in (A) Delta (dashed line) and lower Nooksack (solid line), (B) Upper Nooksack (solid line) and North Fork (dashed line), (C) South Fork (solid line) and upper South Fork (dashed line), and (D) Middle Fork. Transect numbers refer to Figure 1. Scale of vertical and horizontal axes is the same in each panel.

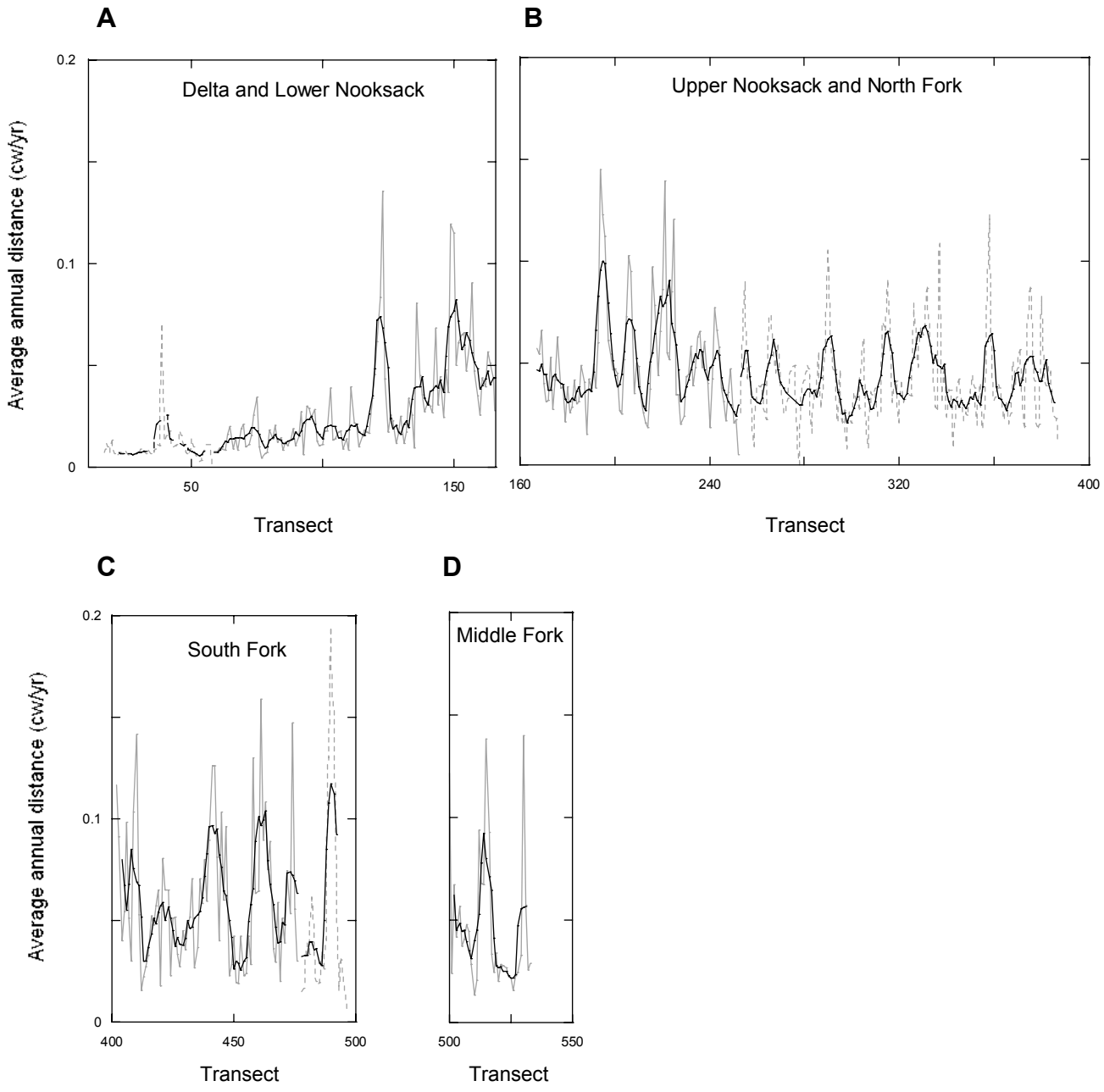

Figure 10. Average annual distance of lateral movement, for the period of aerial photo record (1933-2002), divided by the width of the active channel in 1998; distance is expressed as channel widths per year. Darker line represents a 1-km moving average of the 0.2-km spaced transect data. (A) Delta (dashed line) and lower Nooksack (solid line), (B) Upper Nooksack (solid line) and North Fork (dashed line), (C) South Fork (solid line) and upper South Fork (dashed line), and (D) Middle Fork. Transect numbers refer to Figure 1. Scale of vertical and horizontal axes is the same in each panel.

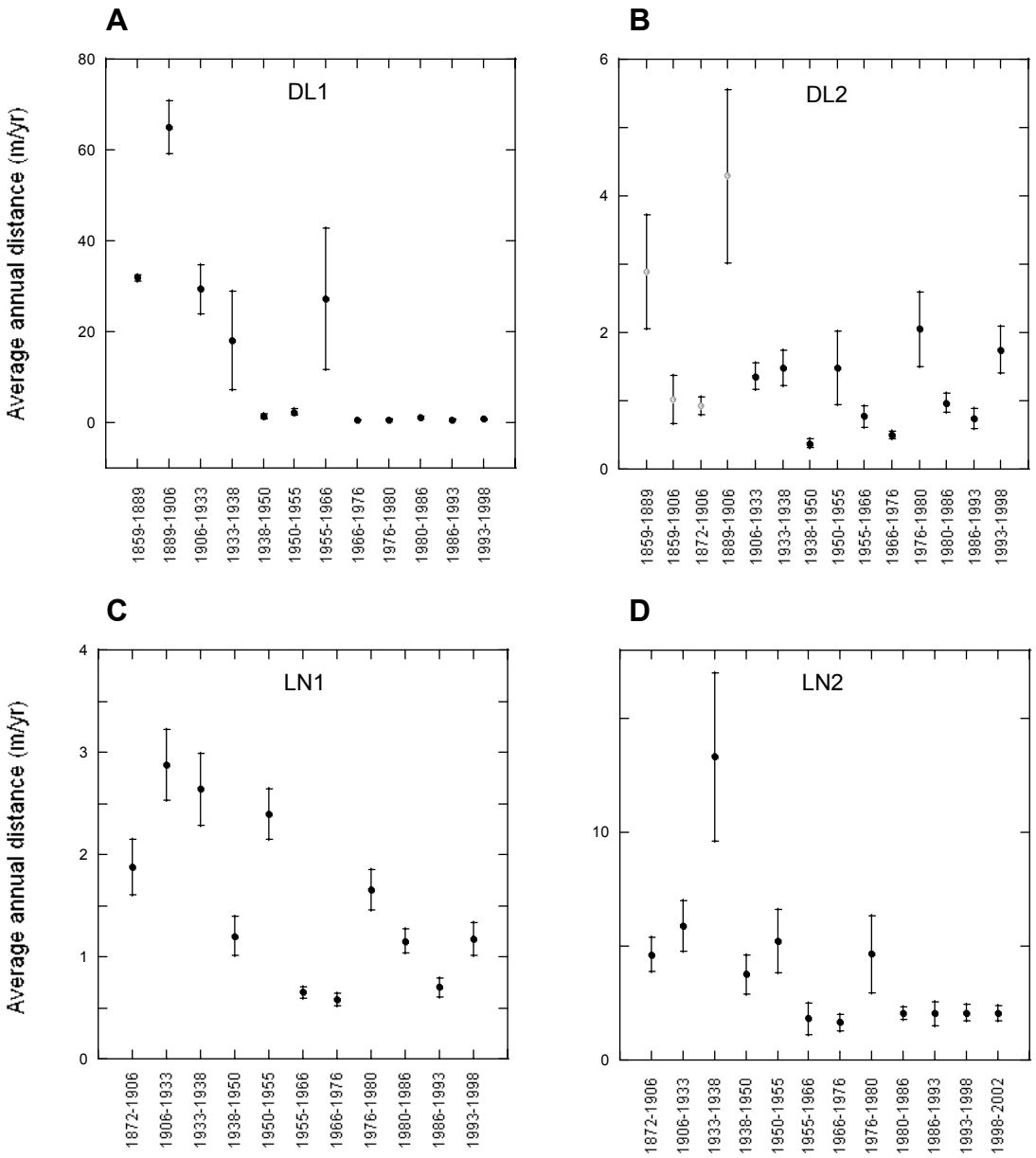

Figure 11 (continued on following pages). Mean annual rate and 1 standard error of channel movement, averaged for time periods, for study segments. A: Delta 1 (D1), B: Delta 2 (D2), C: Lower Nooksack 2 (LN1), D: Lower Nooksack 2 (LN2). Time periods having open symbol in panel B represent time periods that overlap and having different sample sizes. Scale of vertical axis varies between panels.

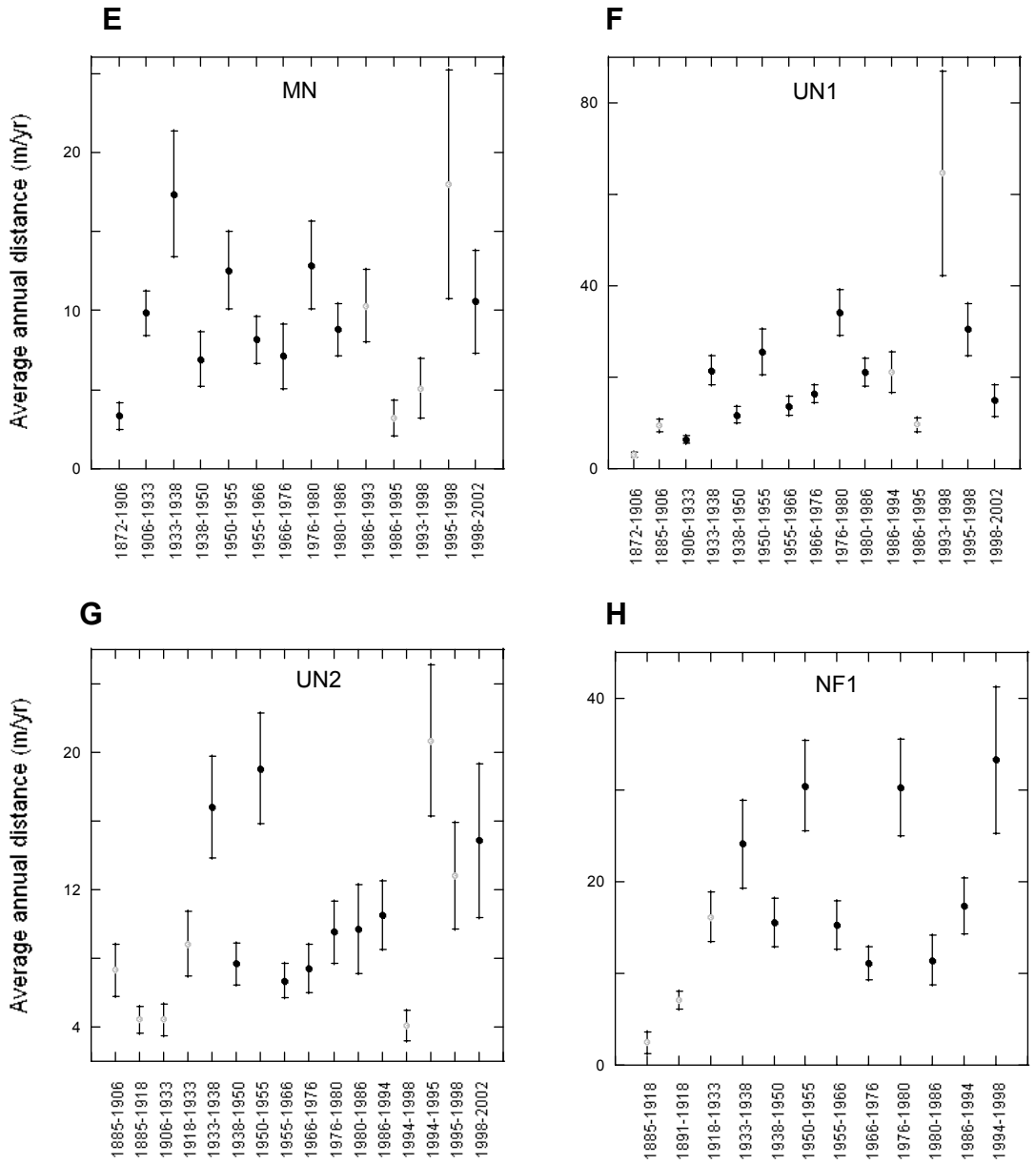

Figure 11 (continued from previous page and on following page). Mean annual rate (and 1 standard error) of channel movement, averaged for time periods, for study segments. E: Middle Nooksack (MN); F: Upper Nooksack 1 (UN1); G: Upper Nooksack 2 (UN2); H: North Fork 1 (NF1). Time periods having open symbol in panel B represent time periods that overlap and having different sample sizes. Scale of vertical axis varies between panels.

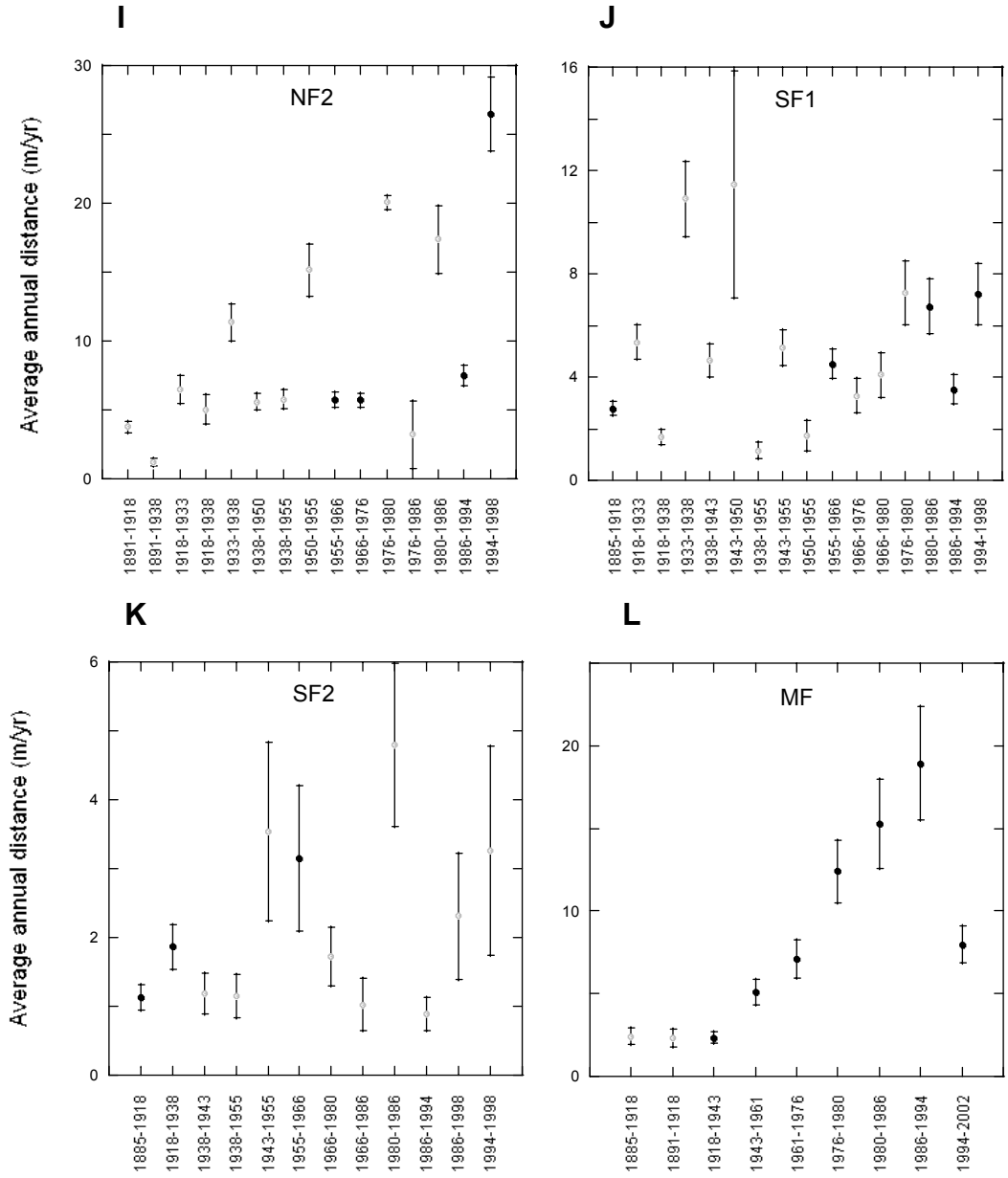

Figure 11 (continued from previous page). Mean annual rate (and 1 standard error) of channel movement, averaged for time periods, for study segments. I: North Fork 2 (NF2); J: South Fork 1 (SF1); K: South Fork 2 (SF2); L: Middle Fork (MF). Time periods having open symbol in panel B represent time periods that overlap and having different sample sizes. Scale of vertical axis varies between panels.

Table 5. Time-weighted, average annual migration rates, measured along transects shown in Figure 1, and averaged for study segments described in Table 1. Migration rate is mean and standard deviation, in meters; sample size (n) is the number of transects. Three columns represent, from left to right, the entire period of map and photo record, for maps prior to the photo record, and for photo record beginning in 1933, respectively.

SEGMENT	ALL YEARS (m/yr ± SD)	< 1933 (m/yr ± SD)	1933-2002 (m/yr ± SD)
Delta 1 (n=13; n=6 <1933))	14.1 ± 12.0	34.3 ± 6.1	7.0 ± 12.6
Delta 2 (n=35)	1.3 ± 0.9	1.3 ± 1.6	0.9 ± 0.8
Lower Nooksack 1 (n=57)	1.6 ± 1.0	2.3 ± 2.1	1.2 ± 0.6
Lower Nooksack 2 (n=29)	4.1 ± 2.6	5.2 ± 4.1	3.5 ± 3.1
Middle Nooksack (n=22)	7.6 ± 3.2	6.2 ± 4.5	9.1 ± 4.0
Upper Nooksack 1 (n=47)	13.2 ± 5.7	7.4 ± 4.8	17.2 ± 7.8
Upper Nooksack 2 (n=39)	8.4 ± 4.1	5.8 ± 4.0	10.3 ± 5.5
North Fork 1 (n=82)	14.2 ± 9.1	9.3 ± 5.0	18.5 ± 8.6
North Fork 2 (n=125)	6.7 ± 3.9	3.9 ± 3.8	8.3 ± 5.5
Middle Fork (n=34)	6.6 ± 4.6	2.9 ± 2.6	9.2 ± 6.3
South Fork 1 (n=96)	4.8 ± 3.0	3.3 ± 2.7	5.4 ± 3.9
South Fork 2 (n=20)	2.8 ± 1.5	1.5 ± 0.9	4.2 ± 3.4

PATTERNS OF HISTORICAL FLOODPLAIN OCCUPANCY

Figure 12 shows an occupation grid for the study area, for the entire period of record, and Figure 13 shows the same grid for the aerial photo era (1933-2002) only. The grids show the percent of the record during which each 2-m cell was occupied by the active channel (i.e., low flow and high flow channels) and floodplain sloughs. In other words, if twelve sets of aerial photos or maps cover a particular 2-m cell, and the active river or a floodplain slough occupied that cell six of the possible twelve times, then the "percent of years occupied" is fifty percent.

In Figure 12 in the Lower Delta (DL1) segment, notable grid patterns reflect shifting flow amounts between distributary channels, and also the outward progradation of delta channels. The pattern in the Upper Delta (DL2) segment reflects the very low rates of lateral migration both before diking and after diking (approximately 1 m/yr; see Table 5). The grid pattern in the downstream part of the lower Nooksack (segment LN1) reflects migration primarily by the outward and downstream translocation of meanders. While the meandering pattern is obvious in the upper part of the lower Nooksack (LN2), the grid pattern primarily reflects the effects of meanders having been cutoff and the channel straightened during the period of record.

A second type of pattern is apparent in the middle Nooksack (MN), which is transitional in migration characteristics between the lower and middle Nooksack. In the Middle Nooksack, and particularly in the upper Nooksack (UN1 and UN2), the grid pattern is consistent with a channel-switching avulsion mechanism, rather than the downstream and outward migration, and eventual cutoff, associated with meandering rivers. There are no forested islands within the upper Nooksack that remain during the period of record, although there are patches of less frequent occupation within the high-occupation areas. This absence of forested islands may be because the branching river pattern (and associated forested islands) evident on the GLO plat maps in the upper Nooksack appears as a wide, straight channel by the early topographic maps, consistent with a braided river. A transition from a branching pattern with stable

forested islands to a braided pattern can be caused by riparian logging, which reduces bank integrity and introduces a very large amount of coarse sediment to channels, or with great increases in coarse sediment supply, or with loss of wood sizable enough to form key pieces and wood jams. Investigating the cause of the historic transition to the upper Nooksack's channel is beyond the scope of this project, any or all of these factors may have played a role in the historic transition to the upper Nooksack's pattern.

The grid pattern in the South Fork Nooksack (SF1) reflects a combination of meandering, branching, and braided patterns in different parts of the valley. The zone of historical channel occupation is notably narrower than that of the upper Nooksack, and relative to the width of the valley (see discussion below and Figure 14 and Tables 6 and 7). The North Fork below the Middle Fork (NF1) has a very wide zone of historical occupation, and suggests the combination of branching and braiding of the upper Nooksack. The zone of historical occupation of the upper North Fork (NF2; upstream of the Middle Fork) and the Middle Fork (MF) nearly fill their floodplains, being relatively confined between terraces and landslide deposits.

Several differences are apparent between the grid patterns for the entire period of record (Figure 12) and that for the time of the photo record only (Figure 13). The pattern in the lower delta reflects less avulsion, and in the lower Nooksack, less migration and meander cutoff avulsion, in the latter period compared to the former. Occupation in the upper Nooksack is more confined to a single braided area in the photo period compared to forested islands associated with branching from the GLO plat maps evident in the grid from the entire period of record in Figure 12. To a lesser extent there are indications of this transition in the lower and upper North Fork and the South Fork. The occupation pattern in the Middle Fork is very similar in Figures 12 and 13.

Figure 14A shows the historical channel zone (HCZ) relative to the 1998 floodplain width, for all transects, and as a dimensionless ratio in Figure 14B. The historical channel zone is measured as the outer

limits of the zone in which the active channel (low flow channel and gravel bars) has been present in any of the maps and photos used in this study. This ratio is averaged for the 12 study segments in Table 6.

The data show a very large variation in the amount of the floodplain the channel has historically used. The historical channel zone is only about one-seventh (15%) of the floodplain width in the lower Nooksack, while it is about three-fourths (74%) in the North Fork (Table 6). The channel has also used a relatively large portion of the Middle Fork and upper Nooksack, and a relatively small percentage of the South Fork. Figure 14B also shows the ratio between the historical channel zone and the 1998 active channel width; the width of the historical channel zone ranges between about two and five channel widths. The ratio between the two is lowest in the North Fork and Middle Fork, in part because both have wide, braided channels, and because avulsion is dominated by channel switching. The ratio is largest in the lower Nooksack, in part because the channel is narrow and dominated by migration of large-amplitude meanders.

Figure 12 (seven following pages). Occupation grids for the period of map and aerial photo record (1859-2002). Analysis segments from Table 1 are indicated on individual figures: DL1: Delta 1; DL2: Delta 2; LN1: Lower Nooksack 1; LN2: Lower Nooksack 2; MN: Middle Nooksack; UN1: Upper Nooksack 1; UN2: Upper Nooksack 2; SF1: South Fork 1; NF 1: North Fork 1; MF: Middle Fork; SF2: South Fork 2; NF2: North Fork 2. All panels have a common scale. Background image is mosaiced USGS 7.5' topographic maps. Area shown in white represents the floodplain, as delineated in this study; large Holocene landslides in the North Fork and at the confluence of the North and South forks are shown with cross-hatched pattern; Holocene terraces and alluvial fans are shown with simple hatched pattern. River miles (labeled every fifth river mile) are from USGS topographic maps.

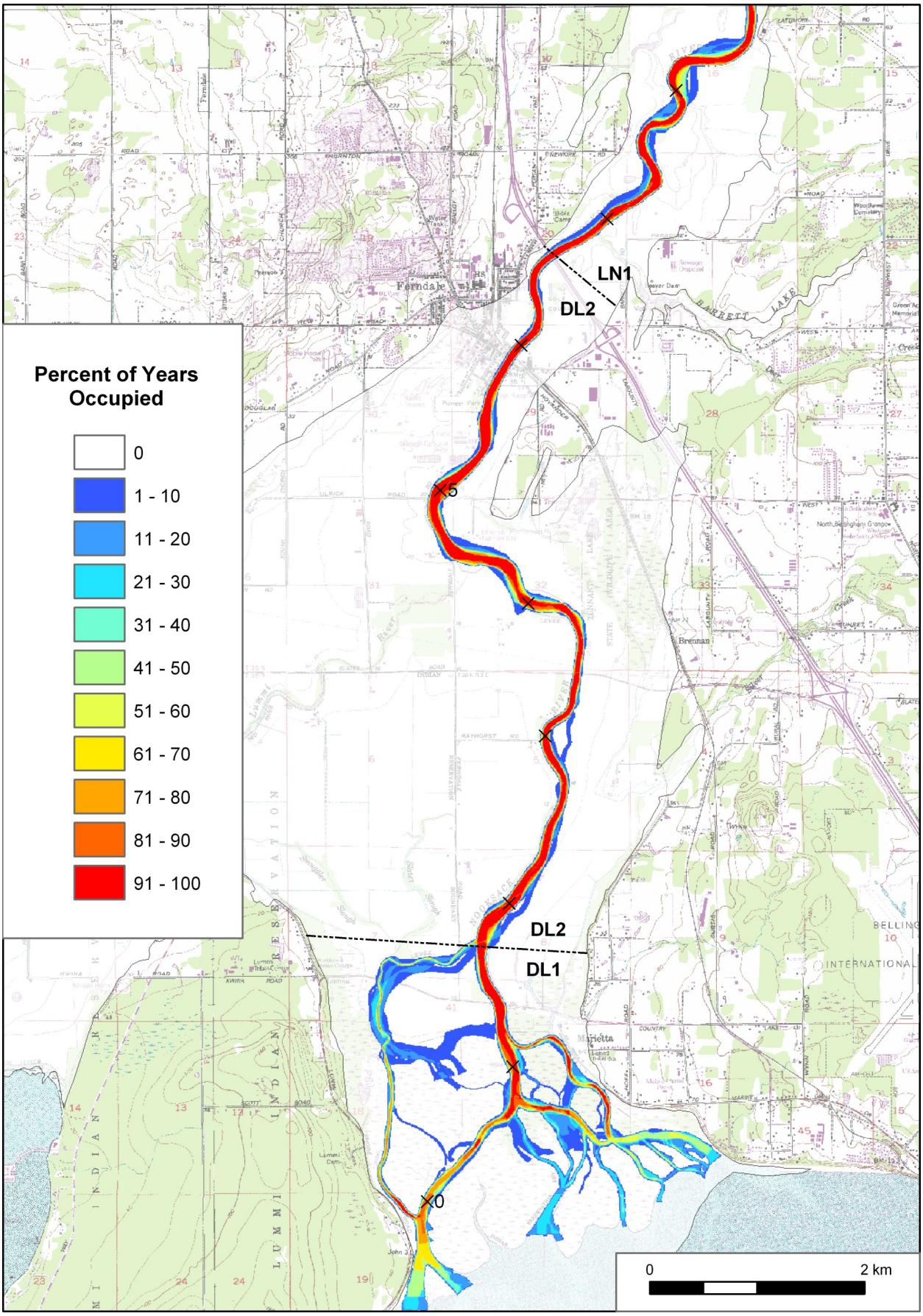
Percent of Years Occupied
0
1 - 10
11 - 20
21 - 30
31 - 40
41 - 50
51 - 60
61 - 70
71 - 80
81 - 90
91 - 100
LN1
DL2
DL2
DL1
5
0
0
2 km

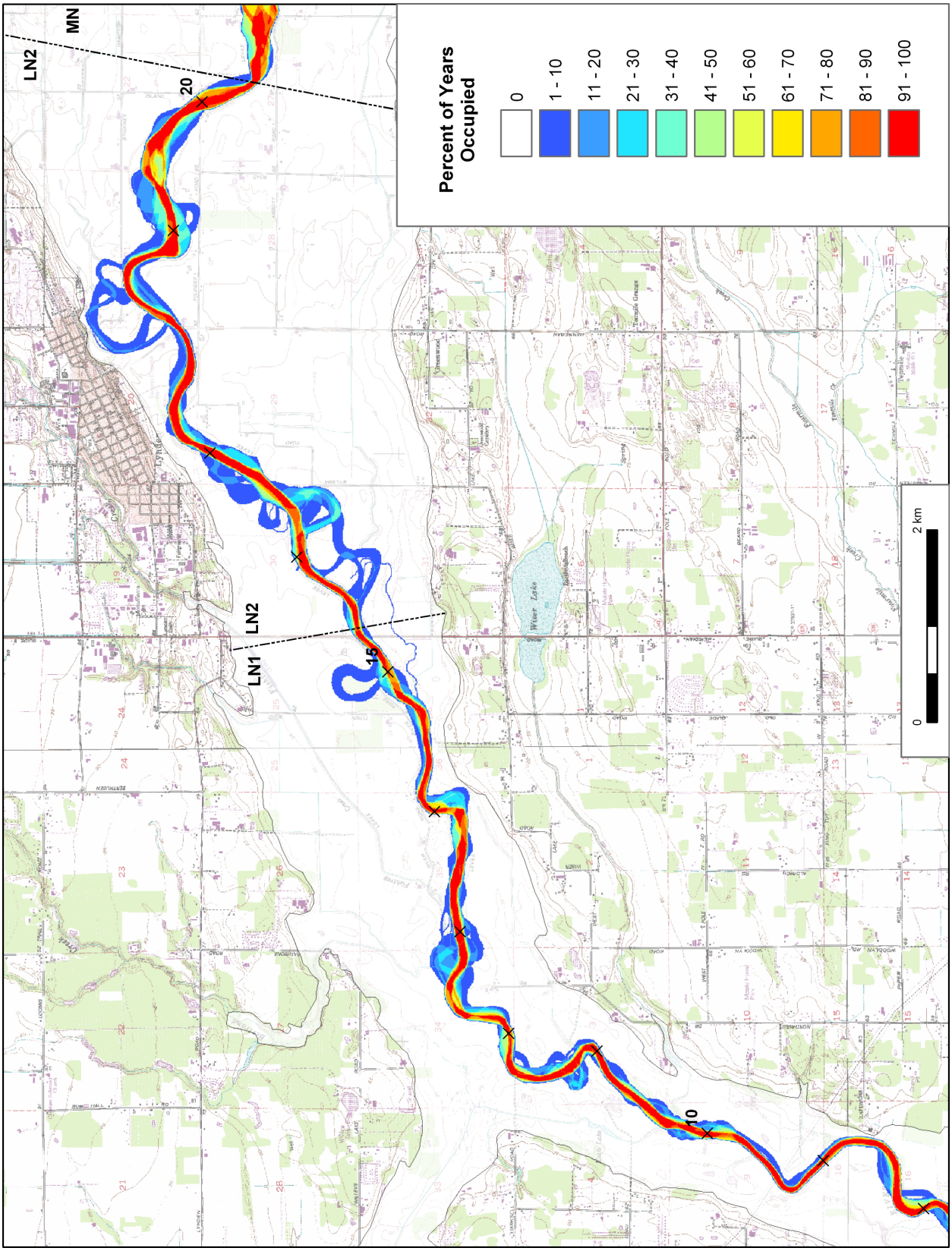
Percent of Years Occupied
0
1 - 10
11 - 20
21 - 30
31 - 40
41 - 50
51 - 60
61 - 70
71 - 80
81 - 90
91 - 100
LN2
MN
20
LN2
LN1
15
10
0
2 km

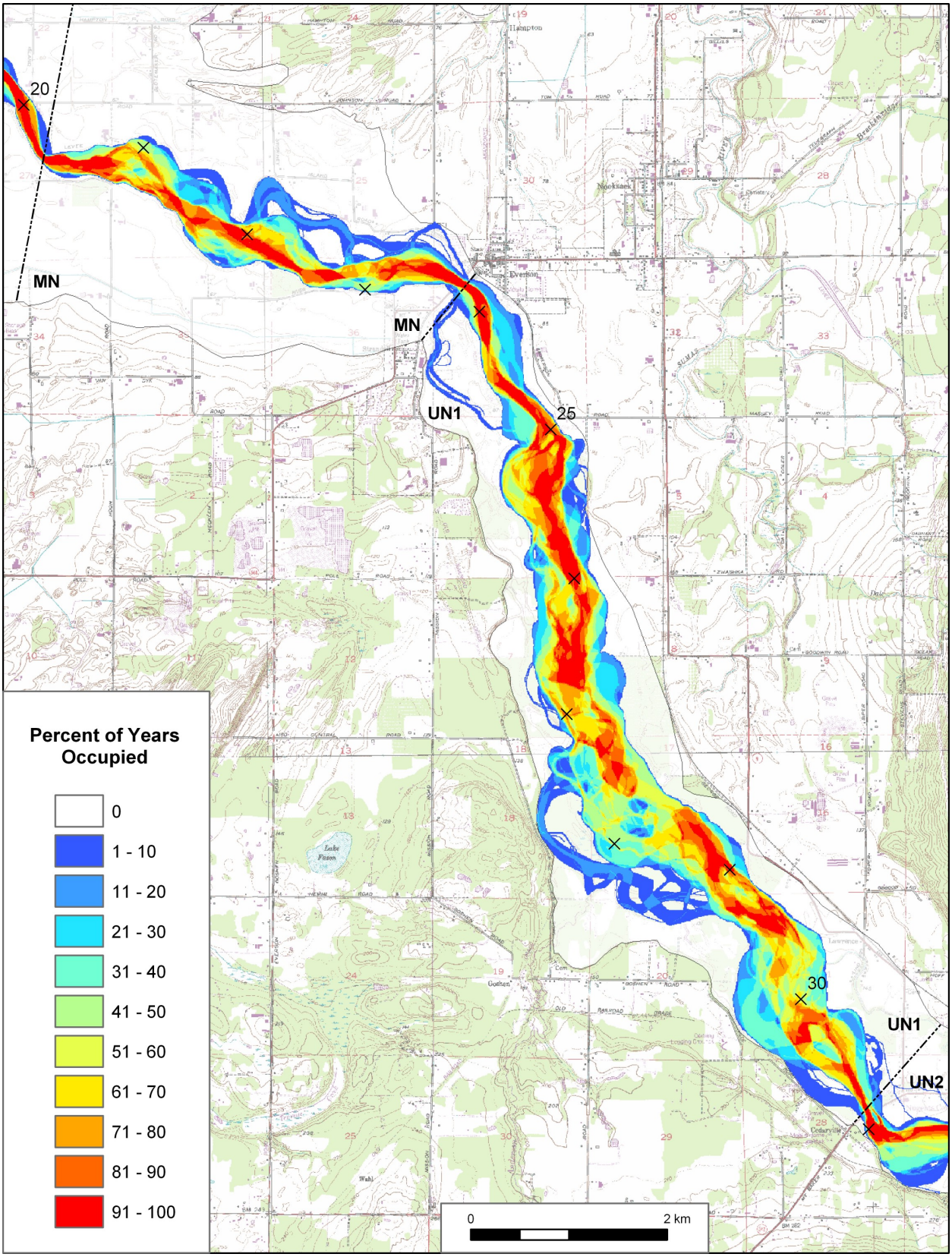
20
MN
MN
UN1
25
30
UN1
UN2
Percent of Years Occupied
0
1 - 10
11 - 20
21 - 30
31 - 40
41 - 50
51 - 60
61 - 70
71 - 80
81 - 90
91 - 100
0
2 km